Drug Metab. Pharmacokinet. 26 (3): 256–265 (2011).

Regular Article

Interpretation of the Effects of Protein Kinase C Inhibitors on Human UDP-glucuronosyltransferase 1A (UGT1A) Proteins *in cellulo*

Yuko ABE, Ryoichi FUJIWARA, Shingo ODA, Tsuyoshi YOKOI and Miki NAKAJIMA*

Drug Metabolism and Toxicology, Faculty of Pharmaceutical Sciences, Kanazawa University, Kanazawa, Japan

Full text of this paper is available at http://www.jstage.jst.go.jp/browse/dmpk

Summary: UDP-glucuronosyltransferases (UGTs) catalyze the glucuronidation of a wide variety of xeno/endobiotics. Previous studies have reported that human UGT enzymes are phosphorylated and that treatment of cells with protein kinase C (PKC) inhibitors results in decreased UGT activities without affecting the UGT protein levels. In this study, we investigated the effects of PKC inhibitors on human UGT1A protein levels and activities in detail. When UGT1A-expressing HEK293 cells and LS180 cells were treated with curcumin or calphostin C, the exogenous and endogenous UGT1A protein levels in homogenates prepared with Tris-buffered saline were significantly decreased. Enzyme activity levels mirrored the changes in UGT protein levels. When the curcumin- or calphostin C-treated cells were lysed with buffer containing a detergent, the UGT protein levels did not decrease. We found that curcumin or calphostin C treatment facilitated the degradation of UGT protein after the cells were collected in the absence of a detergent. Finally, by *in cellulo* evaluation, we found that curcumin decreased UGT activity by the direct inhibitory effect, but calphostin C did not affect UGT activity. Thus, this study suggests that we should evaluate the data carefully when interpreting the effects of PKC inhibitors on UGT activity.

Keywords: UGT; glucuronidation; phosphorylation; degradation; inhibition

Introduction

UDP-glucuronosyltransferases (UGTs; EC 2.4.1.17) are a superfamily of enzymes that catalyze the conjugation of endogenous and exogenous compounds with UDP-glucuronic acid (UDPGA) as a cosubstrate.[1] UGT enzymes are localized to the endoplasmic reticulum membrane. The transmembrane domain is near the carboxyl terminus and most of the mass is on the luminal side.[2] Human UGTs are subdivided into two families, UGT1 and UGT2, based on amino acid sequence identity. To date, 19 individual UGT isoforms have been identified in humans.[3] These isoforms have different or overlapping substrate specificities and show tissue-specific expressions.

Protein phosphorylation is one of the most common protein modifications. Previous studies have reported that the phosphorylation event affects UGT activity: Basu *et al.*[4] first reported that the treatment of LS180 cells, HT-29 cells, or UGT1A1-expressing COS-1 cells with curcumin and calphostin C, which are potent inhibitors of protein kinase C (PKC), decreased glucuronosyltransferase activities toward bilirubin and anthraflavic acid without affecting UGT protein levels. They demonstrated that UGT1A1 incorporated [^{33}P]orthophosphate, which was inhibited by calphostin C. Mutations in predicted phosphorylation sites of UGT1A1 (T75A, T112A, and S435G) resulted in decreased enzyme activities. In 2004, Basu *et al.* found similar results for human UGT1A10, which is expressed in the gastrointestinal tract.[5] Subsequently, they reported that overexpression or inhibition of PKCε, as well as mutation of the predicted phosphorylation sites, altered the substrate preference of UGT1A7.[6] In 2008, they reported that treatment of LS180 cells with calyculin A, a phosphatase inhibitor I, or PKC agonists such as 1,2-dihexanoyl-*sn*-glycerol, facilitated restoration of UGT activity.[7]

In this study, we examined the effects of curcumin and calphostin C on the activities and protein levels of UGTs *in vitro* and *in cellulo*. We treated UGT1A1-, UGT1A4-, UGT1A6-, UGT1A7-, and UGT1A9-expressing HEK293 cells and LS180 cells, which endogenously express UGT enzymes, with curcumin and calphostin C. We found a significant inconsistency between the previous studies and our current work, and noted that we should evaluate the data carefully when interpreting the effects of PKC inhibitors on UGT activity.

Received; December 10, 2010, Accepted; January 28, 2011
J-STAGE Advance Published Date: February 8, 2011, doi:10.2133/dmpk.DMPK-10-RG-121
**To whom correspondence should be addressed:* Miki NAKAJIMA, Ph.D., *Drug Metabolism and Toxicology, Faculty of Pharmaceutical Sciences, Kanazawa University, Kanazawa 920-1192, Japan. Tel. +81-76-234-4407, Fax. +81-76-234-4407, E-mail: nmiki@p.kanazawa-u.ac.jp*

Materials and Methods

Chemicals and reagents: UDPGA, alamethicin, 4-methylumbelliferone (4-MU), leflunomide, MG-132, and wortmannin were purchased from Sigma-Aldrich (St. Louis, MO). Curcumin, calphostin C, and genistein were purchased from Wako Pure Chemicals (Osaka, Japan). Caspase inhibitor I and calpain inhibitor *N*-acetyl-leucyl-leucyl-norleucinal (ALLN) were purchased from Merck (Darmstadt, Germany). Rabbit anti-human UGT1A polyclonal antibody was obtained from BD Gentest (Woburn, MA). Mouse anti-KDEL monoclonal antibody was obtained from Stressgen (Victoria, Canada). Rabbit anti-human GAPDH antibody was purchased from Imgenex (San Diego, CA).

Cells culture and chemical treatment: HEK293 cells stably expressing human UGT1A1, UGT1A4, UGT1A6, and UGT1A9 were established previously.[8] HEK293 cells stably expressing human UGT1A7 was established by the transfection of an expression vector containing UGT1A7 cDNA.[9] These cells were cultured in Dulbecco's modified Eagle's medium (DMEM) supplemented with 4.5 g/L glucose, 10 mM HEPES, and 10% fetal bovine serum (FBS) (Invitrogen, Carlsbad, CA). LS180 cells were obtained from the American Type Culture Collection (Rockville, MD) and cultured in DMEM supplemented with 10% FBS and 0.1 mM nonessential amino acids (Invitrogen). HEK293 cells and LS180 cells were maintained at 37°C under an atmosphere of 5% CO_2–95% air. The cells were treated with curcumin, calphostin C, genistein, or leflunomide. To inhibit protein degradation systems, the cells were treated with MG-132, wortmannin, chloroquine, ALLN, or caspase inhibitor I for 1 h before the treatment with curcumin or calphostin C. These chemicals, except for chloroquine (which was dissolved in water), were dissolved in dimethyl sulfoxide with a final concentration in the medium of less than 0.2%.

Preparation of cell homogenate: Cells were suspended in Tris-buffered saline (TBS) [25 mM Tris-HCl buffer (pH 7.4), 138 mM NaCl, and 2.7 mM KCl] and disrupted by freeze-thawing three times as described previously.[8] The suspensions were homogenized by 10 strokes with a Teflon-glass homogenizer. In some cases, the cells were lysed with 0.2% sodium dodecyl sulfate (SDS) or 1% Triton X-100 in TBS. The protein concentrations were determined by Bradford assay.[10]

Immunoblot analysis: UGT protein levels were determined by SDS-polyacrylamide gel electrophoresis (SDS-PAGE) and immunoblotting. Cell homogenates from HEK293 cells and LS180 cells, prepared as described above, were boiled for 3 min in Laemmli sample buffer containing 2-mercaptoethanol. A total of 10 μg (HEK293 cells) or 50 μg (LS180 cells) of proteins were separated on a 10% polyacrylamide gel[11] and transferred onto a polyvinylidene difluoride membrane (Immobilon-P, Millipore, Bedford, MA). The membrane was blocked in 3% nonfat dry milk in phosphate-buffered saline (PBS) containing 0.1% Tween 20 at room temperature for 3 h. The membrane was incubated with rabbit anti-human UGT1A polyclonal antibody (1:500, PBS) overnight at room temperature. Biotinylated anti-rabbit IgG and a VECTSTAIN ABC kit (Vector Laboratories, Burlingame, CA) were used for diaminobenzidine staining.

Reverse transcriptase-polymerase chain reaction analysis: Total RNA was extracted from HEK293 cells expressing UGT1A9 or LS180 cells using ISOGEN (Nippon Gene, Tokyo, Japan). Reverse transcriptase-polymerase chain reaction (RT-PCR) analyses for UGT1A9, UGT1A1, and glyceraldehyde-3-phosphate dehydrogenase (GAPDH) were performed as described previously.[12] The PCR products (15 μl) were analyzed by electrophoresis with 2% agarose gel and visualized by ethidium bromide staining.

Enzyme assays: 4-MU *O*-glucuronide formation was determined as described previously[8] with slight modifications. Briefly, a typical incubation mixture (200 μl total volume) contained 50 mM Tris-HCl buffer (pH 7.4), 10 mM $MgCl_2$, 2.5 mM UDPGA, 25 μg/ml alamethicin, 0.1 mg/ml total cell homogenate, and 10 μM 4-MU. The reaction was initiated by the addition of UDPGA after a 3-min preincubation at 37°C. After incubation at 37°C for 15 min, the reaction was terminated by the addition of 100 μl of cold methanol. After removal of the protein by centrifugation at 13,000*g* for 5 min, a 20-μl portion of the sample was subjected to HPLC. The HPLC apparatus and conditions were described previously.[8]

For the inhibition study, the concentrations of 4-MU and curcumin ranged from 1–40 μM and 0.05–0.5 μM, respectively. Dixon plots were used for the determination of the type of inhibition. Kinetic parameters were determined by nonlinear regression analysis using appropriate software (K-cat, BioMetallics, Princeton, NJ).

For the *in cellulo* glucuronidation assay, cells were incubated with culture medium containing 10 μM 4-MU for 2 h at 37°C. After incubation, a 200-μl portion of the medium was collected and extracted with an equal volume of chloroform. After centrifugation at 13,000*g* for 5 min, a 20-μl portion of the supernatant was subjected to HPLC.

Determination of curcumin concentration in culture media: After curcumin was added at a final concentration of 30 μM, a 100-μl portion of medium was collected at various times. To the media, 4 volumes of acetonitrile were added and vigorously mixed. After centrifugation at 15,000*g* for 5 min, the supernatant was subjected to HPLC. HPLC was performed using an L-7100 pump (Hitachi, Tokyo, Japan), an L-7485 FL detector (Hitachi), an L-7200 autosampler (Hitachi), a D-2500 integrator (Hitachi), and a Symmetry column (4.6 mm × 150 mm, 5 μm; Waters, Milford, MA). The flow rate was 1 mL/min and the column temperature was 35°C. Detection was accomplished with a florescence detector

at 420-nm excitation and 540-nm emission. The mobile phase was 40% acetonitrile adjusted to pH 3.0 with formic acid.

Immunoprecipitation assay: Anti-UGT1AC antibody,[13] an antibody against the common C-terminal region of UGT1A protein, was a generous gift from Dr. Shin-ichi Ikushiro (Toyama Prefectural University, Toyama, Japan). HEK293 cells expressing UGT1A9 cells were treated with curcumin or calphostin C for 1 h and lysed with a buffer containing 1% triton X-100, 0.2% SDS, and 2 mM EDTA. Immunoprecipitation was performed using anti-UGT1AC antibody as described previously,[8] and the immunoprecipitates were subjected to immunoblot analysis using anti-UGT1A, anti-phosphoserine, anti-phosphothreonine, or anti-phosphotyrosine antibodies (ZYMED Laboratories, San Francisco, CA).

Pro-Q Diamond phosphoprotein staining of purified His-tagged UGT1A9: A pFastBac plasmid containing histidine (His)-tagged UGT1A9 cDNA[14] was kindly provided by Dr. Moshe Finel (University of Helsinki, Helsinki, Finland). The recombinant baculovirus was infected to insect cells, and the produced His-tagged UGT1A9 was purified using Ni-NTA Agarose (Qiagen, Hilden, Germany) as described previously.[14] The purified protein was subjected to staining using a Pro-Q Diamond phosphoprotein gel stain kit (Invitrogen). Silver staining and immunoblot analysis using anti-His antibody (Qiagen) were also performed to confirm the purification.

Results

Curcumin and calphostin C decrease UGT protein levels: HEK293 cells expressing human UGT1A1 were treated with curcumin or calphostin C for 1 h, and cell homogenates were prepared using TBS. On immunoblot analysis, we found that UGT1A1 protein levels were dramatically decreased by treatment with curcumin and with calphostin C in a dose-dependent manner (**Fig. 1A**). The same phenomenon was observed for UGT1A4, UGT1A6, UGT1A7, and UGT1A9. In contrast, the expression levels of glucose regulated protein (GRP) 94 and GRP78, which are localized in the endoplasmic reticulum membrane like UGTs, and GAPDH were not affected. These results suggested that curcumin and calphostin C specifically decreased the UGT1A protein levels. Calphostin C is a specific inhibitor of PKC, whereas curcumin inhibits tyrosine kinase as well as PKC.[15] Therefore, we investigated the effects of tyrosine kinase inhibitors on UGT1A protein levels. Treatment with genistein or leflunomide for 1 h did not affect UGT1A protein levels.

LS180 cells were used to investigate the effects on endogenous UGT1A proteins (**Fig. 1B**). Since multiple UGT1A isoforms are expressed in LS180 cells, we evaluated the overall protein level of UGT1As using anti-UGT1A antibody. We found that UGT1A protein levels decreased on treatment with curcumin or calphostin C in a dose-dependent manner (**Fig. 1B**), but GRP94, GRP78, and GAPDH protein levels did not decrease. Also, tyrosine kinase inhibitors did not affect UGT1A protein levels. These results suggest that curcumin and calphostin C specifically decrease UGT1A protein levels irrespective of the isoforms or exogenous or endogenous protein expression.

Curcumin and calphostin C do not affect UGT1A mRNA levels: We investigated whether UGT1A mRNA levels are affected by treatment with curcumin or calphostin C (**Fig. 2**). RT-PCR analysis revealed that UGT1A9 mRNA levels in the HEK293 expression system (**Fig. 2A**) and UGT1A1 mRNA levels in LS180 cells (**Fig. 2B**) were not affected by treatment with curcumin or calphostin C. These results suggest that the decrease of UGT1A protein levels by curcumin or calphostin C treatment was not caused by the suppression of transcription.

Effects of curcumin or calphostin C on UGT1A protein varies with the treatment time: We examined UGT1A protein levels as well as UGT1A activity after treatment with 30 μM curcumin or 100 nM calphostin C for various times (1 min, 0.25, 0.5, 1, 2, 6, 12, and 24 h). When HEK293 cells expressing UGT1A9 were treated with curcumin, the UGT1A9 protein level fell below the detection limit after only a 1-min incubation (**Fig. 3A**). The loss of UGT1A9 protein continued up to 12 h of incubation. Interestingly, the UGT1A9 protein level slightly recovered on 24-h treatment. When the cells were treated with calphostin C, the UGT1A9 protein level fell to 60% of the control with a 1-min treatment, and gradually decreased in a time-dependent manner until 24 h. When LS180 cells were treated with curcumin, the UGT1A protein level fell to 5% of control on a 1-min treatment (**Fig. 3A**). After 15 min of treatment, the UGT1A protein level fell below the detection limit. This reduction continued up to 2 h of treatment. The UGT1A protein level was markedly restored (60–100% of control) when the cells were treated for 6–24 h. When the cells were treated with calphostin C, the UGT1A protein level fell to 50% of the control with a 1-min treatment, and gradually decreased in a time-dependent manner until 24 h. 4-MU *O*-glucuronosyltransferase activities of total cell homogenates prepared from HEK293 cells and from LS180 cells were modified by treatment with curcumin and calphostin C in parallel with changes in UGT1A protein levels (**Fig. 3B**).

Concerning the restoration of the UGT protein level after longer incubation periods with curcumin, we surmised that the concentration of curcumin in the media might decrease during the culture because it has been reported that curcumin is metabolized by UGTs.[16] As shown in **Figure 3C**, we found that the concentration of curcumin in the HEK293 cell medium fell to 60% of control after 6 h of incubation, and gradually decreased thereafter (46% and 16% of control at 12- and 24-h incubations). The fall in concentration of curcumin in the LS180 cell medium was faster than that in the HEK293 cell medium. These results

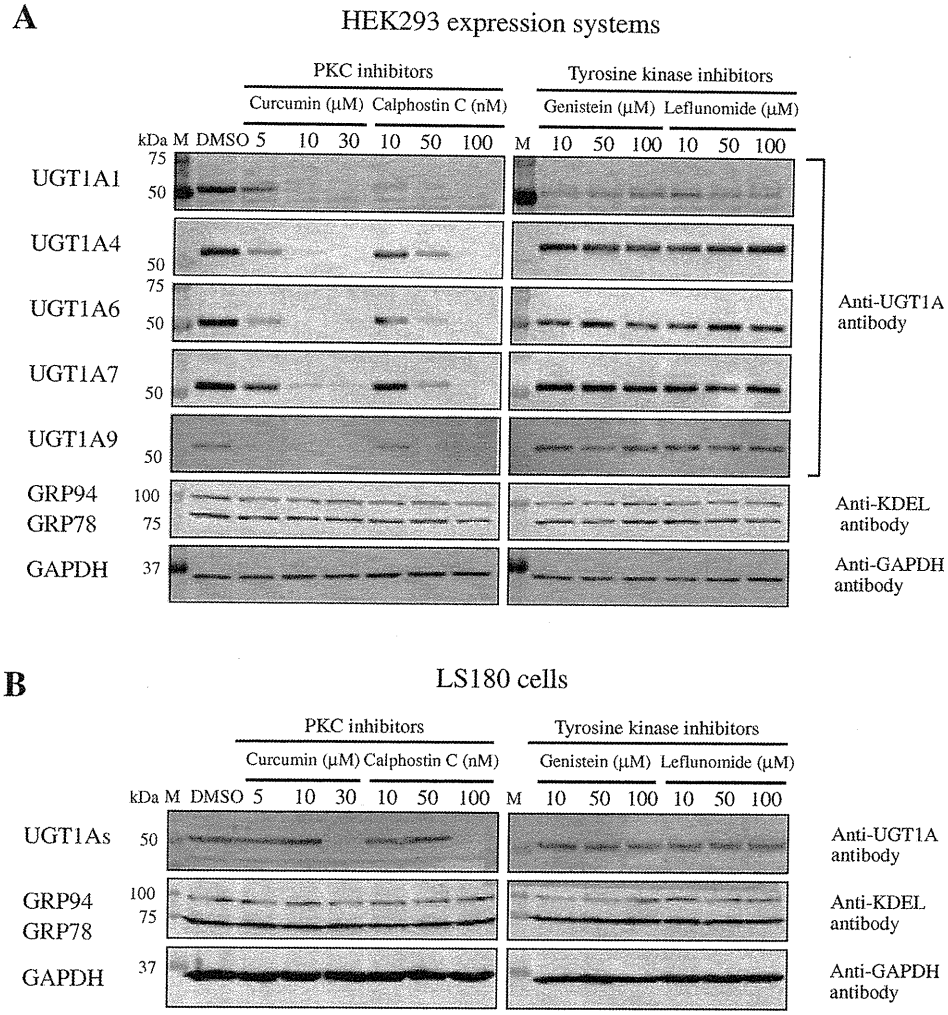

Fig. 1. Effects of PKC inhibitors and tyrosine kinase inhibitors on UGT1A protein levels
HEK293 cells expressing UGT1A1, UGT1A4, UGT1A6, UGT1A7, and UGT1A9 (A) and LS180 cells (B) were treated with curcumin, calphostin C, genistein, or leflunomide. After 1-h treatments, the cells were suspended in TBS and cell homogenates were prepared as described in Materials and Methods. Immunoblot analysis was performed using anti-UGT1A, anti-KDEL, and anti-GAPDH antibodies. M, marker.

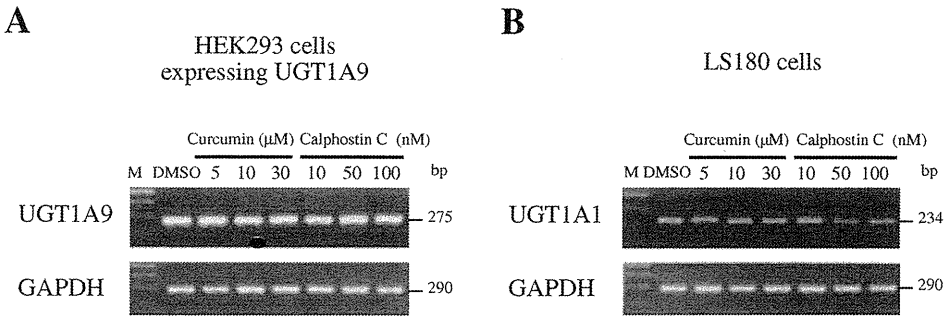

Fig. 2. Effects of curcumin and calphostin C on UGT1A9 mRNA in HEK293 cells and UGT1A1 mRNA in LS180 cells
Total RNA was extracted from cells treated with curcumin or calphostin C for 1 h. RT-PCR analysis was performed for UGT1A9 or UGT1A1 as well as GAPDH. M, marker.

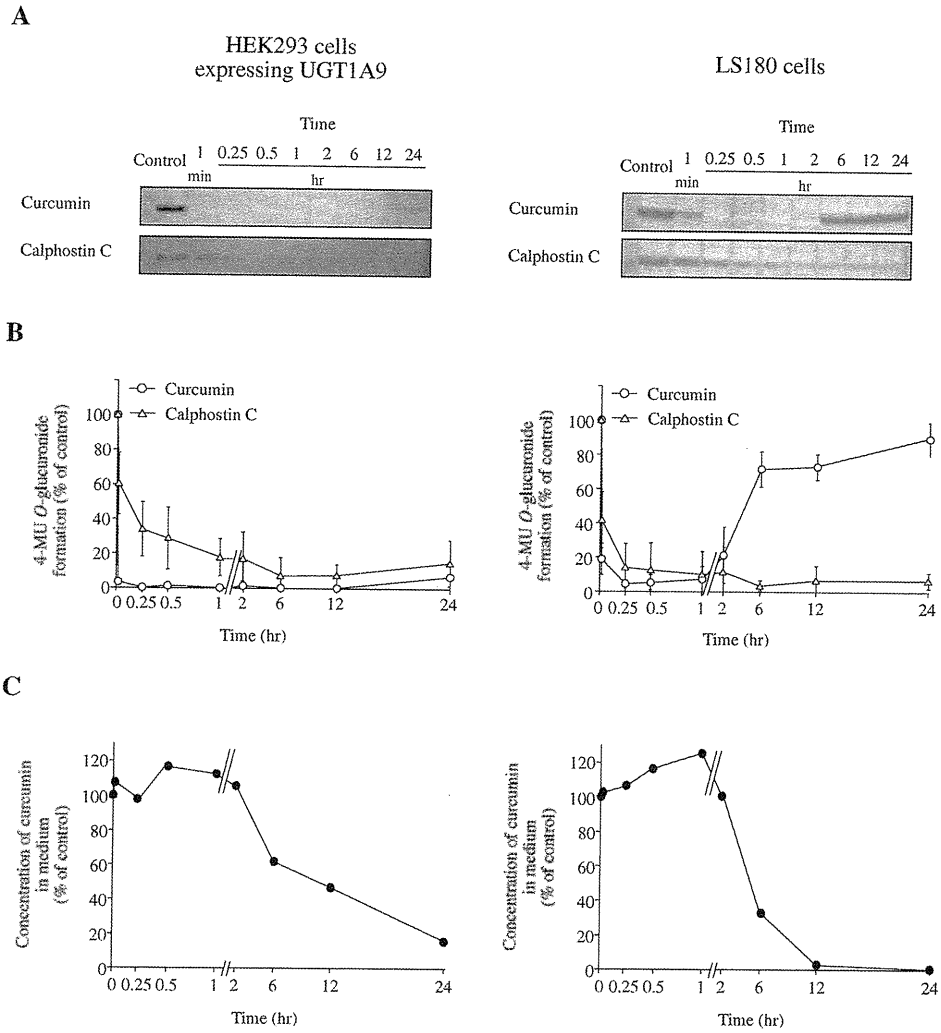

Fig. 3. Effects of curcumin and calphostin C on UGT1A proteins (A) and activities (B) in HEK293 cells and LS180 cells, and remaining curcumin concentrations in the medium (C)

HEK293 cells expressing UGT1A9 and LS180 cells were treated with 30 μM curcumin or 100 nM calphostin C for 1 min, 0.25, 0.5, 1, 2, 6, 12, or 24 h. Total cell homogenates were prepared and subjected to SDS-PAGE followed by immunoblot analysis with anti-UGT1A antibody (A). Using total cell homogenates, 4-MU *O*-glucuronosyltransferase activity was determined. The control activities of the total cell homogenates from HEK293 cells stably expressing UGT1A9 and LS180 cells were 4.3 nmol/min/mg protein and 0.9 nmol/min/mg protein, respectively (B). The remaining curcumin concentration in the cell culture medium was also determined by HPLC after the addition (time 0) of curcumin at a final concentration of 30 μM (C).

suggest that the restoration of UGT proteins was caused by the decrease of curcumin levels in the medium.

Proteasomes, autophagy, and protease inhibitors did not inhibit the loss of UGT1A9 protein: We suspected that the decrease of UGT1A protein on treatment with curcumin or calphostin C might be due to the acceleration of protein degradation. Proteasomes, autophagy, and proteases are major contributing factors of protein degradation. We treated HEK293 cells expressing UGT1A9 with inhibitors of proteasomes (MG-132), autophagy (chloroquine and wortmannin), and proteases (calpain inhibitor ALLN and caspase inhibitor I) for 2 h, and then treated the cells with 30 μM curcumin or 100 nM calphostin C for the last 1 h. However, these inhibitors did not stop the reduction of UGT1A9 protein levels by curcumin or calphostin C (**Fig. 4**). Additionally, we investigated the effects of other protease inhibitors such as *p*-amidinophenylmethanesulfonyl fluoride, trypsin inhibitor, leupeptin, aprotinin, and bestatin on the reduction of UGT1A9 protein levels; however, none of them could inhibit the degradation of UGT1A9 protein (data not shown). This data indicates that the reduction of UGT1A9 protein levels by curcumin or calphostin C was not mediated by proteasomes, autophagy, or proteases.

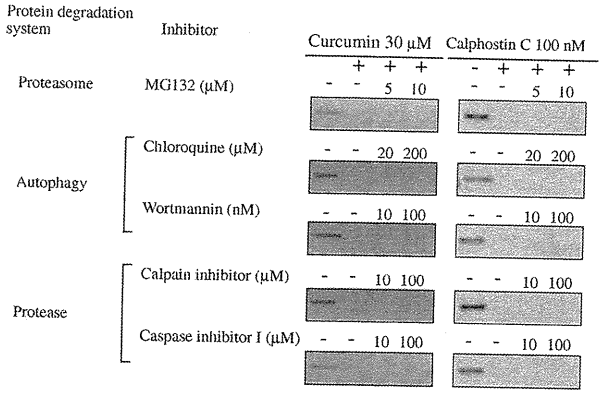

Fig. 4. Effects of proteasome, autophagy, and protease inhibitors on the degradation of UGT1A9 in curcumin- or calphostin C-treated HEK293 cells

After HEK293 cells expressing UGT1A9 were treated with MG132, chloroquine, wortmannin, calpain inhibitor, and caspase inhibitor I for 1 h, the cells were treated with curcumin or calphostin C for 1 h in the presence of these inhibitors. Total cell homogenates were prepared and subjected to SDS-PAGE followed by immunoblot analysis with anti-UGT1A antibody.

The loss of UGT1A protein by curcumin and calphostin C was not observed when the cells were collected with buffer containing a detergent: It was a surprising finding that UGT1A protein levels fell after only 1 min of treatment with curcumin (**Fig. 3A**). After the treatment, we collected the cells with TBS and prepared total cell homogenates by a conventional method for UGT studies. It takes approximately 2 h to finish the preparation of the cell homogenates. We surmised that UGT1A protein might be degraded during the preparation of the cell homogenates. To examine this hypothesis, we directly suspended the cells with Laemmli sample buffer containing 1.5% SDS[11] after treatment with curcumin for 1 h. When the cell lysate was used for the immunoblot analysis, the fall in UGT1A protein levels on curcumin treatment was not observed (**Fig. 5A**). We confirmed that UGT1A protein levels were not decreased by curcumin when the treated cells were suspended with 0.2% SDS or 1% Triton X-100. These results suggest that the degradation of UGT1A proteins by curcumin occurs after the collection of the treated cells.

Next, we sought to investigate when UGT1A protein starts to degrade after the collection of curcumin-treated cells. HEK293 cells expressing UGT1A9 or LS180 cells were treated with 30 μM curcumin for 1 h. Then, the cells were washed and collected with TBS and kept on ice. Just after the collection or 15, 30 min, 1, and 2 h after incubation on ice, the Laemmli sample buffer was added. By the immunoblot analysis of these samples, it was demonstrated that UGT1A9 in HEK293 cells and UGT1As in LS180 cells started to decrease after 1 h on ice (**Fig. 5B**). These results indicate that degradation of the UGT protein by curcumin occurs after the cells are collected. In addition, when the cell homogenates were incubated with curcumin and calphostin C, we didn't see any change of UGT protein levels (data not shown). Therefore, it was indicated that the degradation of UGT occurs only in cells treated with PKC inhibitors.

Effects of curcumin or calphostin C on UGT1A proteins and activities *in cellulo*: As shown in **Figure 3**, we investigated the time-dependency of the effects of curcumin and calphostin C on the UGT1A protein. However, the data should be carefully interpreted, because it was found that the change in the UGT1A protein levels occurred after the cells were collected. To understand the actual effects of curcumin and calphostin C on UGT1A protein levels, we performed immunoblot analysis using cell lysates directly prepared with the Laemmli sample buffer. We found that UGT1A9 levels in HEK293 cells and levels of UGT1As in LS180 cells were not changed (**Fig. 6A**). Next, we evaluated UGT activities *in cellulo* by adding a substrate to the medium and measuring the metabolite formed in the medium, because the cell lysates using the Laemmli sample

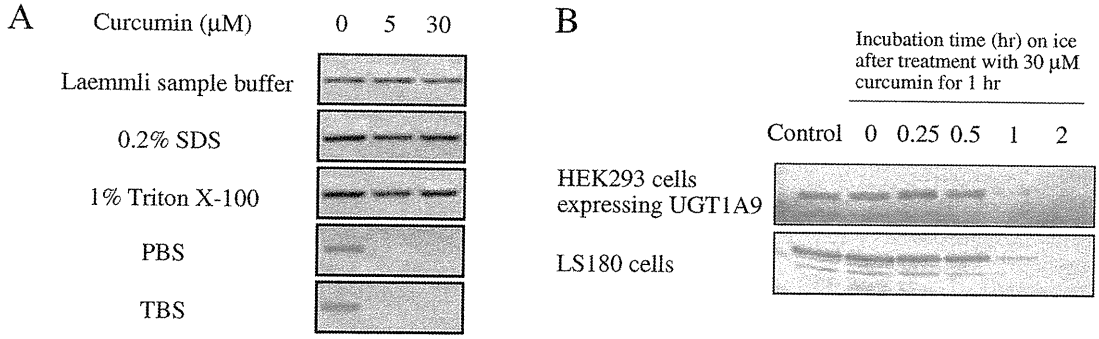

Fig. 5. Degradation of UGT in curcumin- or calphostin C-treated cells did not occur when the cells were collected with a buffer containing a detergent

HEK293 cells expressing UGT1A9 were treated with curcumin for 1 h. The cells were collected with Laemmli sample buffer, 0.2% SDS, 1% Triton X-100, PBS, or TBS, and subjected to SDS-PAGE followed by immunoblot analysis with anti-UGT1A antibody (A). The curcumin-treated HEK293 cells were washed and collected with TBS and kept on ice. Just after the collection (time 0), 0.25, 0.5, 1, or 2 h after the incubation on ice, the Laemmli sample buffer was added and immunoblot analysis was performed with anti-UGT1A antibody (B).

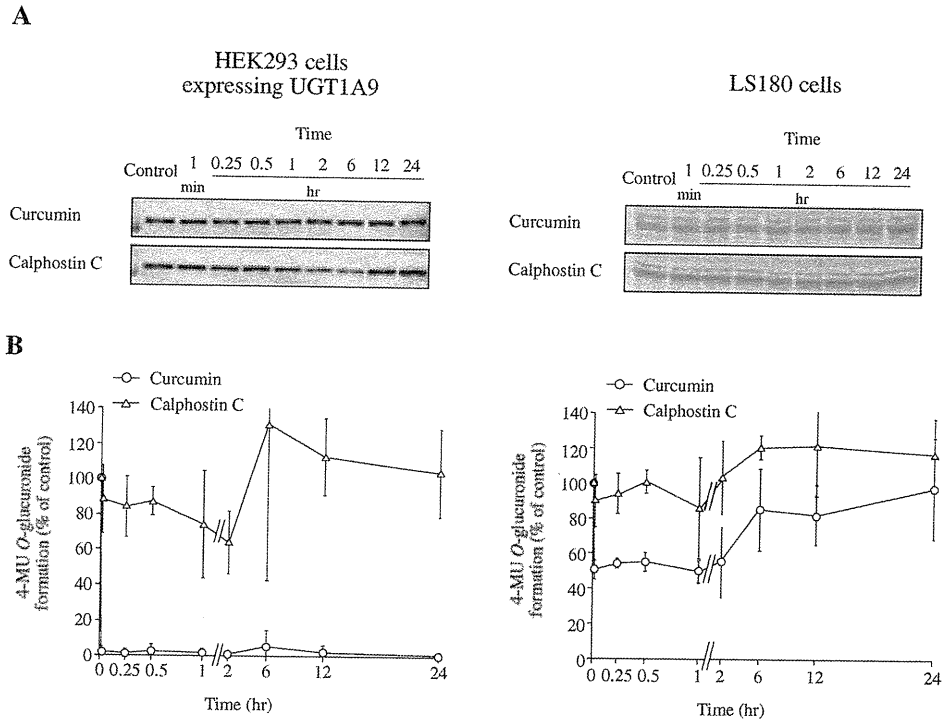

Fig. 6. UGT1A protein levels (A) and activities (B) evaluated *in cellulo* after treatment of the cells with curcumin or calphostin C
HEK293 cells expressing UGT1A9 and LS180 cells were treated with 30 μM curcumin or 100 nM calphostin C for 1 min, 0.25, 0.5, 1, 2, 6, 12, or 24 h. Cells were lysed with Laemmli sample buffer and immunoblot analysis was performed with anti-UGT1A antibody (A). UGT activities in the curcumin- or calphostin C-treated cells were evaluated *in cellulo*. 4-MU was added to the cell culture medium at a final concentration of 10 μM. After 2 h of incubation, the amount of 4-MU *O*-glucuronide in the medium was measured by HPLC (B). Data are mean ± SD (n = 3).

buffer could not be used for measurement of the enzyme activity. When the HEK293 and LS180 cells were treated with calphostin C, no significant change was observed in 4-MU *O*-glucuronide formation (**Fig. 6B**). In contrast, the 4-MU *O*-glucuronide formation in HEK293 cells expressing UGT1A9 was dramatically decreased in the presence of curcumin, and that in LS180 cells was decreased by 50% of control (up to 2 h of treatment) and by 20% (6–12 h of treatment) in the presence of curcumin.

Curcumin inhibits UGT1A9 activity: Since curcumin is a substrate for UGT enzymes, we speculated that the decreases of UGT activities *in cellulo* might be due to inhibition by curcumin. We examined the inhibitory effects of curcumin on 4-MU *O*-glucuronosyltransferase activity by total cell homogenates prepared from HEK293 cells expressing UGT1A9. It was demonstrated that curcumin potently (Ki = 0.26 μM) inhibited UGT1A9 activity in a noncompetitive manner (**Fig. 7**). Thus, the reduction in 4-MU glucuronidation activities by curcumin *in cellulo* is likely due to the direct inhibitory potency of curcumin toward UGT1A9.

Immunoprecipitation assay with anti-UGT1A antibody followed by immunoblotting with anti-phosphoserine, anti-phosphothreonine, or anti-phosphotyrosine antibodies: To examine whether the degradation of UGT proteins by curcumin and by

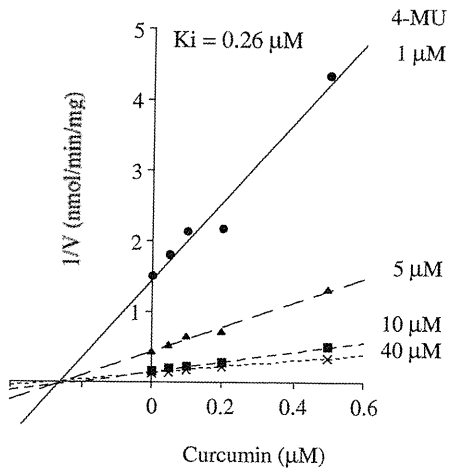

Fig. 7. Inhibitory effects of curcumin on 4-MU *O*-glucuronosyltransferase activity in cell homogenates from HEK293 cells expressing UGT1A9
The concentrations of 4-MU and curcumin were in the ranges 1–40 μM and 0.05–0.5 μM, respectively.

calphostin C treatment links with the decrease in the phosphorylation status of the UGT proteins, we carried out an immunoprecipitation assay (**Fig. 8**). Curcumin- or calphostin C-treated HEK293 cells expressing UGT1A9

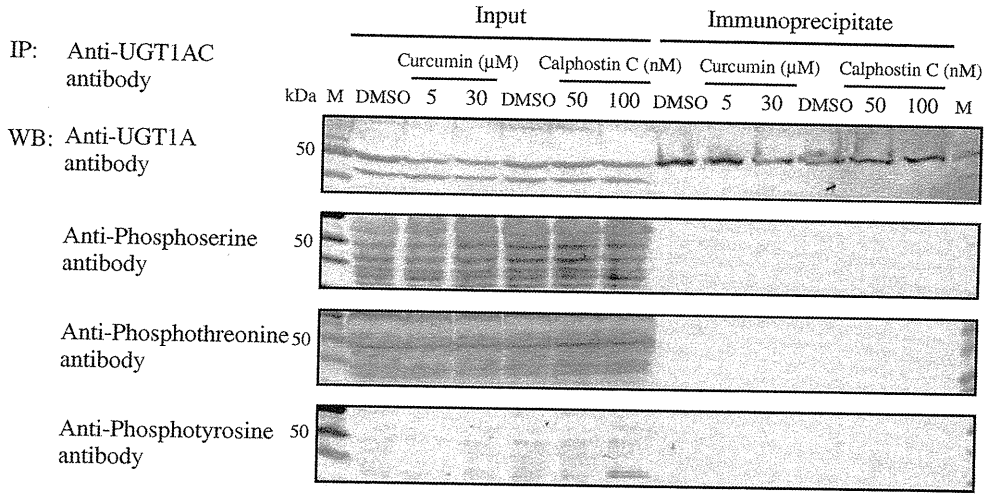

Fig. 8. Immunoprecipitation of UGT1A9 expressed in HEK293 cells and immunoblot analysis
HEK293 cells expressing UGT1A9 were treated with curcumin (5 or 30 μM) or calphostin C (50 or 100 nM) for 1 h. Cells were lysed with a buffer containing 1% Triton X-100, 0.2% SDS, and 2 mM EDTA and immunoprecipitation was performed using anti-human UGT1AC antibody. The immunoprecipitates were subjected to immunoblot analysis using anti-UGT1A, anti-phosphoserine, anti-phosphothreonine, or anti-phosphotyrosine antibodies. As controls, input proteins were also subjected to the immunoblot analysis. IP, immunoprecipitation; WB, Western blot; M, marker.

were lysed with a buffer containing 1% Triton X-100, 0.2% SDS, and 2 mM EDTA and subjected to immunoprecipitation using anti-UGT1AC antibody followed by immunoblotting with anti-UGT1A, anti-phosphoserine, anti-phosphothreonine, or anti-phosphotyrosine antibodies. UGT1A9 protein was successfully immunoprecipitated, but no phosphorylated UGT protein was detected. Thus, this experiment could not prove that UGT1A9 is phosphorylated. In addition, in the input protein, no obvious change was observed in the band pattern of phosphoprotein on curcumin or calphostin C treatment.

Pro-Q Diamond phosphoprotein staining of purified His-tagged UGT1A9: To further investigate whether UGT1A9 is phosphorylated, we carried out Pro-Q Diamond phosphoprotein staining of UGT1A9 protein. His-tagged UGT1A9 was purified using Ni-NTA Agarose and subjected to SDS-PAGE and silver staining, Pro-Q Diamond phosphoprotein staining, or immunoblot analysis with anti-His antibody. As shown in **Figure 9**, a band corresponding to His-tagged UGT1A9 was stained with the Pro-Q Diamond phosphoprotein gel stain kit, indicating that UGT1A9 protein was phosphorylated. However, in this experiment, we could not examine whether curcumin or calphostin C treatment had decreased the phosphorylation status because we prepared the membrane fraction with TBS, which causes degradation of UGT, before the purification step.

Discussion

Basu *et al.*[4–7] reported that the treatment of various cells expressing UGT with curcumin or calphostin C altered glucuronosyltransferase activities. They reported that these PKC inhibitors inhibited the incorporation of [^{33}P]orthophosphate into the UGT protein and decreased UGT activities without changing UGT protein levels. Furthermore, mutations at the predicted phosphorylation sites in UGTs resulted in decreased enzymatic activities. Based on these results, they concluded that the decreased activities were due to inhibition of the phosphorylation of the UGT enzymes. In contrast to their results, we found that UGT protein levels were dramatically decreased on treatment with curcumin or calphostin C (**Figs. 1** and **3**). To examine the reason for the inconsistency, we carefully read their papers and retrospectively noticed differences in the buffers used to prepare the homogenates. Basu *et al.*[4] used TBS, which is usually used for UGT analysis, for the preparation of homogenates to measure enzyme activities. However, for the preparation of cell lysates to perform immunoblot analysis, it seems that they used a buffer containing 1% Triton X-100 and 0.5% SDS.[17] First, we used TBS to prepare cell homogenates for immunoblot analysis and observed a decrease in UGT protein levels. In contrast, when we used buffer containing a detergent to lyse the cells, no decrease in UGT protein levels was observed on treatment with curcumin or calphostin C (**Figs. 5** and **6**). Thus, it should be emphasized that differences in the preparation method of cell homogenates may cause misinterpretation of the results. We concluded that decreased UGT activities on curcumin and calphostin C treatment were due to decreased UGT protein levels. Basu *et al.*[4] determined the effects of PKC inhibitors on UGT in LS180 and UGT-expressing COS-1 cells, and we determined those effects in LS180 and UGT-expressing HEK293 cells. In other words, the data from LS180 cells can be used as a

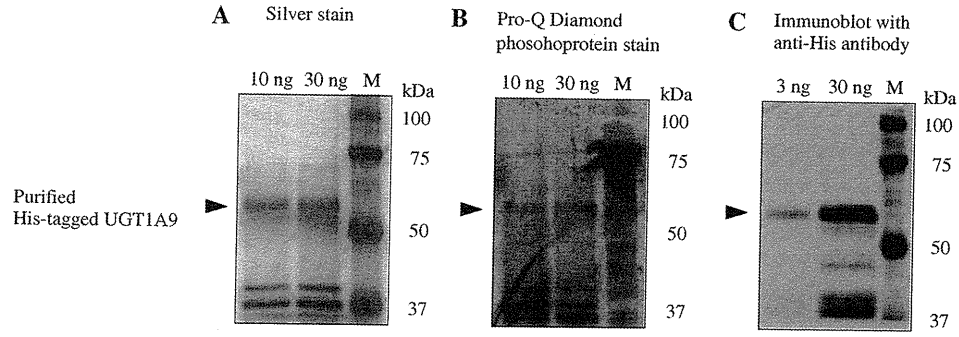

Fig. 9. Pro-Q Diamond phosphoprotein staining of purified His-tagged UGT1A9
Insect cells expressing His-tagged UGT1A9 were collected with TBS and a membrane fraction was prepared. The protein was purified using Ni-NTA Agarose and subjected to silver staining (A), Pro-Q Diamond phosphoprotein staining (B), or immunoblot analysis using anti-His antibody (C). M, marker.

reference between the two studies. Both studies found that the effects of PKC inhibitors were common to endogenous and exogenous UGTs. Therefore, we consider that the inconsistency was not due to the possibility that there are differences in signal transduction including the PKC system between the different cell lines.

To prepare cell homogenate, cells suspended in TBS were disrupted by freeze-thawing three times before homogenization. This is a common method for UGT analysis to elicit enzyme activity. One may question whether the freeze-thawing might possibly make UGT sensitive to PKC inhibitor-caused degradation. However, as shown in **Figure 5B**, when the curcumin-treated cells were lysed directly with Laemmli sample buffer without freeze-thawing, the degradation of UGT protein was still observed after the cells were kept on ice for 1 h. Thus, it is unlikely that freeze-thawing affected the degradation of UGT proteins resulting from treatment with PKC inhibitors. We found that UGT protein levels in the curcumin- or calphostin C-treated cells started to decrease 1 h after collection in the absence of detergents. We suspected that curcumin or calphostin C might facilitate the degradation of UGT proteins through proteasomes, autophagy, and proteases. However, we could not find evidence supporting this hypothesis (**Fig. 4**). Another possibility is that curcumin or calphostin C may decrease translation. However, since the machinery of translation is likely common for all proteins, the hypothesis would not explain the UGT-specific decrease. The underlying mechanism of the decrease of UGT protein levels by curcumin or calphostin C remains to be clarified.

To examine the actual effects of PKC inhibitors on UGT activities, we evaluated the activities *in cellulo*. Curcumin inhibited 4-MU *O*-glucuronidation activity by 50% at most in LS180 cells, but completely inhibited activity in HEK293 cells (**Fig. 6B**). We confirmed using cell homogenates from HEK293 cells expressing UGT1A9 that curcumin is a potent inhibitor of UGT1A9 (**Fig. 7**). Therefore, the inhibitory effects of curcumin on UGT activities seem to be independent of the inhibition of phosphorylation. LS180 cells express multiple UGT isoforms,[12] including UGT1A1 and UGT1A10, which showed high efficiency in terms of curcumin metabolism.[16] Thus, it is considered that the milder inhibitory effects of curcumin in LS180 cells compared to HEK293 cells could be due to the rapid elimination of curcumin in LS180 cells, as shown in **Figure 3C**. In contrast to curcumin, calphostin C did not affect UGT activity *in cellulo*. It has been reported that calphostin C treatment decreased [^{33}P]orthophosphate-labeled UGT1A protein levels.[4] Taken together, it seems that the phosphorylation status of UGT proteins does not significantly affect their enzymatic activities *in cellulo*. Although Basu *et al.*[4,5] reported that mutations at the predicted phosphorylation sites decreased UGT enzyme activities, the possibility that amino acid change *per se*, not the phosphorylation status, may change the enzyme activity cannot be excluded. To determine whether the UGT proteins are phosphorylated, we performed several experiments. An immunoprecipitation assay for UGT1A9 expressed in HEK293 cells using anti-UGT1AC antibody did not show the phosphorylation of UGT1A9 (**Fig. 8**). We also performed a Phos-tag SDS-PAGE analysis[18] using UGT1A9 expressed in HEK293 cells to investigate the phosphorylation status, but no evidence of phosphorylation was revealed (data not shown). Next, we performed Pro-Q Diamond phosphoprotein staining of purified His-tagged UGT1A9 and found that it was phosphorylated (**Fig. 9**). However, when the purified protein was subjected to LC-MS/MS analysis using a NanoFrontier eLD (Hitachi, Tokyo, Japan), no phosphorylated peptide was detected (data not shown). Therefore, a likely explanation is that, even if UGTs are originally phosphorylated, the extent of phosphorylation may not be so high.

During the process of preparing this report, another group reported the role of PKCδ in the functional activity of human UGT1A6.[19] They reported that rottlerin (a PKCδ selective inhibitor) and non-selective PKC inhibitors (calphostin C, curcumin, and hypericin) decreased acetamin-

ophen glucuronidation in LS180 cells by more than 50%. Although they did not observe an increase of serotonin glucuronidation in Sf9 cells expressing UGT1A6 on treatment with PKC activators such as phorbol myristate acetate and 1-oleoyl-2-acetyl-sn-glycerol, they found that co-expression of PKCδ increased the protein-normalized UGT1A6 activity in HEK293T cells. However, it remains to be examined whether the phosphorylation status of UGT1A6 was actually increased by the co-expression of PKCδ.

In conclusion, we found that the treatment of cells with curcumin and calphostin C resulted in a decrease of UGT protein levels. The degradation was observed only after the cells were collected with a buffer not containing a detergent. Even if the cells continued to be cultured in the presence of calphostin C, *in cellulo* UGT activity and protein levels were not affected. Thus, this study revealed that we should evaluate the data carefully when interpreting the effects of PKC inhibitors on UGT activity.

Acknowledgements: We thank Dr. Moshe Finel for providing the pFastBac plasmid containing His-tagged UGT1A9 cDNA and Dr. Shin-ichi Ikushiro for providing the anti-UGT1AC antibody. We acknowledge Mr. Brent Bell for reviewing the manuscript.

References

1) Dutton, G. J.: Acceptor substrates of UDP glucuronosyltransferase and their assay. In Dutton, G. J. (ed.): *Glucuronidation of Drugs and Other Compounds*, Boca Raton, FL, CRC Press, 1980, pp. 69–78.
2) Meech, R. and Mackenzie, P. I.: Structure and function of uridine diphosphate glucuronosyltransferases. *Clin. Exp. Pharmacol. Physiol.*, **24**: 907–915 (1997).
3) Mackenzie, P. I., Bock, K. W., Burchell, B., Guillemette, C., Ikushiro, S., Iyanagi, T., Miners, J. O., Owens, I. S. and Nebert, D. W.: Nomenclature update for the mammalian UDP glycosyltransferase (UGT) gene superfamily. *Pharmacogenet. Genomics*, **15**: 677–685 (2005).
4) Basu, N. K., Kole, L. and Owens, I. S.: Evidence for phosphorylation requirement for human bilirubin UDP-glucuronosyltransferase (UGT1A1) activity. *Biochem. Biophys. Res. Commun.*, **303**: 98–104 (2003).
5) Basu, N. K., Kubota, S., Meselhy, M. R., Ciotti, M., Chowdhury, B., Hartori, M. and Owens, I. S.: Gastrointestinally distributed UDP-glucuronosyltransferase 1A10, which metabolizes estrogens and nonsteroidal anti-inflammatory drugs, depends upon phosphorylation. *J. Biol. Chem.*, **279**: 28320–28329 (2004).
6) Basu, N. K., Kovarova, M., Garza, A., Kubota, S., Saha, T., Mitra, P. S., Banerjee, R., Rivera, J. and Owens, I. S.: Phosphorylation of a UDP-glucuronosyltransferase regulates substrate specificity. *Proc. Natl. Acad. Sci. USA*, **102**: 6285–6290 (2005).
7) Basu, N. K., Kole, L., Basu, M., Chakraborty, K., Mitra, P. S. and Owens, I. S.: The major chemical-detoxifying system of UDP-glucuronosyltransferases requires regulated phosphorylation supported by protein kinase C. *J. Biol. Chem.*, **283**: 23048–23061 (2008).
8) Fujiwara, R., Nakajima, M., Yamanaka, H., Nakamura, A., Katoh, M., Ikushiro, S., Sakaki, T. and Yokoi, T.: Effects of coexpression of UGT1A9 on enzymatic activities of human UGT1A isoforms. *Drug Metab. Dispos.*, **35**: 747–757 (2007).
9) Izukawa, T., Nakajima, M., Fujiwara, R., Yamanaka, H., Fukami, T., Takamiya, M., Aoki, Y., Ikushiro, S., Sakaki, T. and Yokoi, T.: Quantitative analysis of UDP-glucuronosyltransferase (UGT) 1A and UGT2B expression levels in human livers. *Drug Metab. Dispos.*, **37**: 1759–1768 (2009).
10) Bradford, M. M.: A rapid and sensitive method for the quantitation of microgram quantities of protein utilizing the principle of protein-dye binding. *Anal. Biochem.*, **72**: 248–254 (1976).
11) Laemmli, U. K.: Cleavage of structural proteins during the assembly of the head of bacteriophage T4. *Nature*, **227**: 680–685 (1970).
12) Nakamura, A., Nakajima, M., Yamanaka, H., Fujiwara, R. and Yokoi, T.: Expression of UGT1A and UGT2B mRNA in human normal tissues and various cell lines. *Drug Metab. Dispos.*, **36**: 1461–1464 (2008).
13) Ikushiro, S., Emi, Y., Kato, Y., Yamada, S. and Sakaki, T.: Monospecific antipeptide antibodies against human hepatic UDP-glucuronosyltransferase 1A subfamily (UGT1A) isoforms. *Drug Metab. Pharmacokinet.*, **21**: 70–74 (2006).
14) Kurkela, M., García-Horsman, J. A., Luukkanen, L., Mörsky, S., Taskinen, J., Baumann, M., Kostiainen, R., Hirvonen, J. and Finel, M.: Expression and characterization of recombinant human UDP-glucuronosyltransferases (UGTs). UGT1A9 is more resistant to detergent inhibition than other UGTs and was purified as an active dimeric enzyme. *J. Biol. Chem.*, **278**: 3536–3544 (2003).
15) Hong, R. L., Spohn, W. H. and Hung, M. C.: Curcumin inhibits tyrosine kinase activity of p185neu and also depletes p185neu. *Clin. Cancer Res.*, **5**: 1884–1891 (1999).
16) Hoehle, S. I., Pfeiffer, E. and Metzler, M.: Glucuronidation of curcuminoids by human microsomal and recombinant UDP-glucuronosyltransferases. *Mol. Nutr. Food Res.*, **51**: 932–938 (2007).
17) Ritter, J. K., Yeatman, M. T., Kaiser, C., Gridelli, B. and Owens, I. S.: A phenylalanine codon deletion at the *UGT1* gene complex locus of a Crigler-Najjar type I patient generates a pH-sensitive bilirubin UDP-glucuronosyltransferase. *J. Biol. Chem.*, **268**: 23573–23579 (1993).
18) Kinoshita, E., Kinoshita-Kikuta, E., Takiyama, K. and Koike, T.: Phosphate-binding tag, a new tool to visualize phosphorylated proteins. *Mol. Cell. Proteomics*, **5**: 749–757 (2006).
19) Volak, L. P. and Court, M. H.: Role for protein kinase C delta in the functional activity of human UGT1A6: implications for drug-drug interactions between PKC inhibitors and UGT1A6. *Xenobiotica*, **40**: 306–318 (2010).

0090-9556/11/3905-838–846$25.00
DRUG METABOLISM AND DISPOSITION

DMD 39:838–846, 2011

Vol. 39, No. 5
37259/3683405
Printed in U.S.A.

DMD

DRUG METABOLISM AND DISPOSITION

CYP2C9-Mediated Metabolic Activation of Losartan Detected by a Highly Sensitive Cell-Based Screening Assay[S]

Atsushi Iwamura, Tatsuki Fukami, Hiroko Hosomi, Miki Nakajima, and Tsuyoshi Yokoi

Drug Metabolism and Toxicology, Faculty of Pharmaceutical Sciences, Kanazawa University, Kanazawa, Japan

Received November 14, 2010; accepted February 14, 2011

ABSTRACT:

Drug-induced hepatotoxicity is a major problem in drug development, and reactive metabolites generated by cytochrome P450s are suggested to be one of the causes. CYP2C9 is one of the major enzymes in hepatic drug metabolism. In the present study, we developed a highly sensitive cell-based screening system for CYP2C9-mediated metabolic activation using an adenovirus vector expressing CYP2C9 (AdCYP2C9). Human hepatocarcinoma HepG2 cells infected with our constructed AdCYP2C9 for 2 days at multiplicity of infection 10 showed significantly higher diclofenac 4′-hydroxylase activity than human hepatocytes. AdCYP2C9-infected cells were treated with several hepatotoxic drugs, resulting in a significant increase in cytotoxicity by treatment with losartan, benzbromarone, and tienilic acid. Metabolic activation of losartan by CYP2C9 has never been reported, although the metabolic activations of benzbromarone and tienilic acid have been reported. To identify the reactive metabolites of losartan, the semicarbazide adducts of losartan were investigated by liquid chromatography-tandem mass spectrometry. Two CYP2C9-specific semicarbazide adducts of losartan (S1 and S2) were detected. S2 adduct formation suggested that a reactive metabolite was produced from the aldehyde metabolite E3179, but a possible metabolite from S1 adduct formation was not produced via E3179. In conclusion, a highly sensitive cell-based assay to evaluate CYP2C9-mediated metabolic activation was established, and we found for the first time that CYP2C9 is involved in the metabolic activation of losartan. This cell-based assay system would be useful for evaluating drug-induced cytotoxicity caused by human CYP2C9.

Introduction

Drug-induced hepatotoxicity is a serious problem in drug development and clinical practice. In the United States, it accounts for more than 50% of cases of acute liver failure, and more than 600 drugs have been associated with hepatotoxicity (Lee, 2003; Park et al., 2005). That is why some drugs that were launched on the market were later withdrawn. Therefore, the prediction of drug-induced hepatotoxicity before clinical trials is important in drug development, and multiple cell-based assays have been developed for evaluation of drug-induced hepatotoxicity (Greer et al., 2010). Sometimes, drug-induced hepatotoxicity is associated with reactive metabolites produced by drug-metabolizing enzymes (Guengerich, 2008). However, species differences in drug-metabolizing enzymes or other factors between humans and laboratory animals are a major problem in predicting the hepatotoxicity.

This work was supported in part by Research on Advanced Medical Technology, Health and Labor Science Research from the Ministry of Health, Labor, and Welfare of Japan [Grant H20-BIO-G001].

Article, publication date, and citation information can be found at http://dmd.aspetjournals.org.

doi:10.1124/dmd.110.037259.

[S] The online version of this article (available at http://dmd.aspetjournals.org) contains supplemental material.

Cytochrome P450 (P450) enzymes are the most studied drug-metabolizing enzymes, accounting for ~75% of the metabolism of clinical drugs (Guengerich, 2008). Among them, CYP3A4 is the predominant isoform expressed in human liver, accounting for up to 60% of the total hepatic P450 protein and responsible for more than 50% of drug metabolism (Guengerich, 2008). To date, many researchers have tried to predict drug-induced hepatotoxicity in vitro using human hepatocarcinoma HepG2 cells, but the low expression levels of P450 enzymes in HepG2 cells may be responsible for the fact that 30% of the compounds were falsely classified as nontoxic (Rodríguez-Antona et al., 2002; Hewitt and Hewitt, 2004). Useful in vitro cell-based assays have been established with HepG2 cells, leading to improved evaluation of drug-induced cytotoxicity. For example, our previous study showed that benzodiazepines such as flunitrazepam and nimetazepam were metabolically activated by CYP3A4 by coincubation with HepG2 cells and CYP3A4 Supersomes (Mizuno et al., 2009). Vignati et al. (2005) demonstrated that various hepatotoxic drugs such as flutamide and troglitazone were activated by CYP3A4 using HepG2 cells transiently transfected with CYP3A4. Thus, the activation of hepatotoxic drugs by CYP3A4 has been well evaluated, but the contribution of other P450 enzymes remains to be evaluated. CYP2C is the second most highly expressed P450 subfamily in human liver, and CYP2C9 is the most highly expressed isoform in this family

ABBREVIATIONS: P450, cytochrome P450; Nrf2, nuclear factor-E2 p-45-related factor; GFP, green fluorescent protein; GAPDH, glyceraldehyde-3-phosphate dehydrogenase; siRNA, small interfering RNA; HPLC, high-performance liquid chromatography; WST-8, 2-(2-methoxy-4-nitrophenyl)-3-(4-nitrophenyl)-5-(2, 4-disulfophenyl)-2*H*-tetrazolium monosodium salt; LC, liquid chromatography; MS/MS, tandem mass spectrometry; LCMS-IT-TOF, liquid chromatography ion trap time-of-flight mass spectrometry; MOI, multiplicity of infection; BSO, buthionine sulfoximine; ALT, alanine aminotransferase; FLU-1, 4-nitro-3-(trifluoromethyl)phenylamine.

(Edwards et al., 1998). CYP2C9 is responsible for the metabolism of various pharmaceutical drugs and appears to be partially involved in the generation of reactive metabolites, as is CYP3A4 (Li, 2002). For example, benzbromarone is metabolized via 6-hydroxybenzbromarone to a catechol by CYP2C9, followed by the oxidization of the catechol to a reactive *ortho*-quinone metabolite (McDonald and Rettie, 2007). Tienilic acid is metabolized to reactive intermediates, the thiophene sulfoxide or the thiophene epoxide, by CYP2C9 (Koenigs et al., 1999). In recent studies, we developed useful in vitro cell-based assays using adenovirus to sensitively evaluate the involvement of CYP3A4 and superoxide dismutase 2 in drug-induced cytotoxicity (Yoshikawa et al., 2009; Hosomi et al., 2010). In the present study, a highly sensitive cytotoxicity assay system for CYP2C9-mediated metabolic activation was established in a similar way, and the drug-induced cytotoxicity was evaluated with the established assay system. Drugs investigated in this study were hepatotoxic drugs that are known to be CYP2C9 substrates (flutamide, fluvastatin, losartan, terbinafine, valproic acid, and zolpidem) and those that are known to be metabolically activated by CYP2C9 (benzbromarone and tienilic acid). As a result, we found for the first time that the cytotoxicity of losartan was enhanced by CYP2C9 and then performed additional studies to identify the structures of the reactive metabolites.

Materials and Methods

Chemicals and Reagents. Diclofenac, fluvastatin, and tienilic acid were obtained from Wako Pure Chemicals (Osaka, Japan). Losartan and terbinafine were obtained from LKT Laboratories (St. Paul, MN). Benzbromarone, flutamide, valproic acid, and zolpidem were obtained from Sigma-Aldrich (St. Louis, MO). Candesartan, eprosartan, irbesartan, telmisartan, and valsartan were obtained from Toronto Research Chemicals (Ontario, ON, Canada). Olmesartan was kindly provided by Daiichi-Sankyo (Tokyo, Japan). 4′-Hydroxydiclofenac and human CYP2C9 and CYP3A4 Supersomes (recombinant cDNA-expressed P450 enzymes prepared from a baculovirus insect cell system) were purchased from BD Gentest (Woburn, MA). The Adenovirus Expression Vector Kit (Dual Version) and adenovirus genome DNA-TPC were obtained from Takara Bio (Shiga, Japan). The QuickTiter Adenovirus Titer Immunoassay Kit was from Cell Biolabs (Tokyo, Japan). Stealth Select RNAi for Nrf2 (accession number NM_006164) and Stealth RNAi Negative Control Medium GC Duplex #2 were obtained from Invitrogen (Carlsbad, CA). Dulbecco's modified Eagle's medium was from Nissui Pharmaceutical (Tokyo, Japan). Restriction enzymes were from New England Biolabs (Ipswich, MA) and Takara Bio. All primers were commercially synthesized at Hokkaido System Sciences (Sapporo, Japan). Other chemicals were of analytical or the highest grade commercially available.

Cell Culture. Human embryonic kidney 293 cells and human hepatocarcinoma HepG2 cells were obtained from American Type Culture Collection (Manassas, VA). The 293 and HepG2 cells were maintained in Dulbecco's modified Eagle's medium containing 10% fetal bovine serum (Invitrogen), 3% glutamine, 16% sodium bicarbonate, and 0.1 mM nonessential amino acids (Invitrogen) in a 5% CO_2 atmosphere at 37°C. Cells were infected with the adenovirus in medium containing 5% fetal bovine serum.

Recombinant Adenovirus. A recombinant adenovirus expressing CYP2C9 (AdCYP2C9) was constructed using the cosmid-terminal protein complex method according to the manufacturer's instructions. CYP2C9 cDNA prepared by reverse transcription-polymerase chain reaction using total RNA from human liver obtained at autopsy was inserted into the SwaI site of the pAxcwtit vector. The use of human liver was approved by the ethics committees of Kanazawa University (Kanazawa, Japan) and Iwate Medical University (Morioka, Japan). The nucleotide sequences of CYP2C9 were confirmed by DNA sequence analysis (Long-Read Tower DNA sequencer; GE Healthcare, Little Chalfont, Buckinghamshire, UK). This vector and the parental adenovirus DNA terminal protein complex were cotransfected into 293 cells by Lipofectamine 2000 (Invitrogen). The recombinant adenovirus was isolated and propagated into the 293 cells. In a similar way, the recombinant adenovirus vector expressing a green fluorescence protein (GFP) was generated in the previous study (Hosomi et al., 2010). Viral titers were determined by a QuickTiter Adenovirus Titer Immunoassay Kit. The titers of AdCYP2C9 and AdGFP were 8.6×10^8 and 2.1×10^8 plaque-forming units/ml, respectively.

Immunoblot Analyses of Human CYP2C9 and Nrf2. SDS-polyacrylamide gel electrophoresis and immunoblot analyses of human CYP2C9, Nrf2, and GAPDH were performed. For human CYP2C9, total cell homogenates from adenovirus-infected HepG2 cells (5 μg) were separated on 7.5% polyacrylamide gels and electrotransferred onto a polyvinylidene difluoride membrane, Immobilon-P (Millipore Corporation, Billerica, MA). The membrane was probed with a polyclonal rabbit anti-human CYP2C9 antibody (Daiichi Pure Chemicals, Tokyo, Japan). Biotinylated anti-rabbit IgG and a VECTASTAIN ABC Kit (Vector Laboratories, Burlingame, CA) were used for diaminobenzidine staining. For human Nrf2, total cell homogenates from siRNA-transfected and adenovirus-infected HepG2 cells (25 μg) were separated on 7.5% polyacrylamide gels and electrotransferred onto a polyvinylidene difluoride membrane, Immobilon-P. The membrane was probed with polyclonal rabbit anti-human Nrf2 antibody (Santa Cruz Biotechnology, Inc., San Diego, CA), and the corresponding fluorescent dye-conjugated second antibody and an Odyssey infrared imaging system (LI-COR Biosciences, Lincoln, NE) were used for detection. For human GAPDH, SDS-polyacrylamide gel electrophoresis and immunoblot analysis were performed according to H. Hosomi, T. Fukami, A. Iwamura, M. Nakajima, and T. Yokoi (manuscript submitted for publication).

Diclofenac 4′-Hydroxylase Activity. HepG2 cells (3×10^5 cells/well) were seeded in 12-well plates. After a 24-h incubation, cells were infected with AdCYP2C9 or AdGFP for 1, 2, 3, or 5 days. Then, after a 1-h incubation with 100 μM diclofenac, the medium was subjected to high-performance liquid chromatography (HPLC) to measure the concentration of 4′-hydroxydiclofenac, a metabolite of diclofenac catalyzed by CYP2C9. The HPLC analysis was performed using an L-2130 pump (Hitachi, Tokyo, Japan), an L-2200 autosampler (Hitachi), and a D-2500 Chromato-Integrator (Hitachi) equipped with a Mightysil RP-18 C18 GP column (5-μm particle size, 4.6 mm i.d. × 150 mm; Kanto Chemical, Tokyo, Japan). The eluent was monitored at 280 nm. The mobile phase was 35% acetonitrile containing 20 mM sodium perchlorate (pH 2.5). The flow rate was 1.0 ml/min. The column temperature was 35°C. The retention times of 4′-hydroxydiclofenac and diclofenac were 8.1 and 22.8 min, respectively. The quantification of 4′-hydroxydiclofenac was performed by comparing the HPLC peak height with that of an authentic standard. The limit of quantification in the reaction mixture for 4′-hydroxydiclofenac was 250 nM with a coefficient of variation of <2%.

Cytotoxicity Assay. Nrf2 is known to regulate cytoprotective genes such as glutathione transferase, heme oxygenase-1, NAD(P)H:quinine oxidoreductase, superoxide dismutase, and UDP-glucuronosyltransferase (Copple et al., 2008). Our recent study demonstrated that drug-induced cytotoxicity could be detected with high sensitivity by the knockdown of Nrf2 in HepG2 cells (H. Hosomi, T. Fukami, A. Iwamura, M. Nakajima, and T. Yokoi, manuscript submitted for publication). Likewise, knockdown of Nrf2 was performed by siRNA transfection in this study. HepG2 cells were transfected with Stealth Select RNAi for Nrf2 (siNrf2) and Stealth RNAi Negative Control Medium GC Duplex #2 (siScramble) by Lipofectamine RNAiMAX Reagent (Invitrogen). According to the manufacturer's protocol, RNAi duplex-Lipofectamine RNAiMAX complexes were prepared and added to each well before the HepG2 cells were seeded (1.0×10^4 cells/well). The concentrations of siNrf2 and siScramble were 10 nM. After 24-h incubation, the cells were infected with AdCYP2C9 or AdGFP. Forty-eight hours after infection, the cells were treated with benzbromarone, tienilic acid, flutamide, fluvastatin, terbinafine, valproic acid, zolpidem, or sartans (candesartan, eprosartan, irbesartan, losartan, olmesartan, telmisartan, or valsartan) for 24 h. After incubation with the drugs, cell viability was quantified by 2-(2-methoxy-4-nitrophenyl)-3-(4-nitrophenyl)-5-(2, 4-disulfophenyl)-2*H*-tetrazolium monosodium salt (WST-8) and ATP assays according to the manufacturer's protocol. The WST-8 assay, which is a modified 3-(4,5-dimethylthiazol-2-yl)-2,5-diphenyltetrazolium assay, was performed using a Cell Counting Kit-8 (CCK-8 kit; Wako Pure Chemicals). After incubation with the drugs for 24 h, CCK-8 reagent was added and the absorbance of WST-8 formazan was measured at 450 nm. The ATP assay was performed using a CellTiter-Glo Luminescent Cell Viability Assay (Promega, Madison, WI). After incubation with the drugs for 24 h, CellTiter-Glo Reagent was added, and the generation of a luminescent signal

was recorded by using a 1420 ARVO MX luminometer (PerkinElmer Life and Analytical Sciences–Wallac Oy, Turku, Finland).

Detection of Semicarbazide Adducts. A typical reaction mixture (final volume of 0.5 ml) contained 100 nM human CYP2C9 or CYP3A4 Supersomes, 50 mM potassium phosphate buffer (pH 7.4), 1 mM NADPH, 10 mM semicarbazide, and 20 μM [^{14}C]losartan. The final concentration of ethanol in the reaction mixture was less than 1%. Incubation was performed at 37°C for 60 min and terminated by addition of 2 ml of ice-cold methanol. After centrifugation at 15,000*g*, the supernatant was subjected to liquid chromatography (LC)-tandem mass spectrometry (MS/MS) (4000 QTRAP; Applied Biosystems, Foster City, CA). An Agilent 1200 (Agilent Technologies, Santa Clara, CA) was used as the liquid chromatograph with an Inertsil ODS-3V column (5-μm particle size, 4.6 mm i.d. × 250 mm; GL Science, Inc., Tokyo, Japan). The column temperature was 40°C. The mobile phase was 10 mM ammonium acetate buffer (A) and acetonitrile (B). The conditions for elution were as follows: 5 to 45% B (0–5 min), 45 to 70% B (5–55 min), 70 to 100% B (55–60 min), and 5% B (60.01–70 min). Linear gradients were used for all solvent changes. The flow rate was 1 ml/min. The liquid chromatograph was connected to a 4000 QTRAP mass spectrometer operated by the enhanced product ion under the positive mode. The turbo gas was maintained at 450°C. Air was used as the nebulizing and turbo gas at 50 psi. Nitrogen was used as the curtain gas at 30 psi. The declustering potential and collision energy were 50 V and 20 V, respectively. The *m/z* 150 to 500 was scanned at the precursor ion (*m/z* 494.2; semicarbazide adducts of losartan hydroxide).

Identification of Semicarbazide Adducts. A liquid chromatography ion trap time-of-flight mass spectrometry (LCMS-IT-TOF) system (Shimadzu, Kyoto, Japan) was used to identify the structures of the semicarbazide adducts of the losartan hydroxide. The incubation mixture was the same as described above. After centrifugation at 15,000*g* for 5 min, the supernatant was subjected to LCMS-IT-TOF using an Inertsil ODS-3 analytical column (5-μm particle size, 4.6 mm i.d. × 250 mm). The LC conditions were the same as described earlier.

Statistical Methods. Data are expressed as means ± S.D. Statistical significance between the two groups was determined by a two-tailed Student's *t* test. $P < 0.05$ was considered statistically significant.

Results

MOI- and Time-Dependent Changes of Diclofenac 4′-Hydroxylase Activity and CYP2C9 Protein Level. To investigate the optimum multiplicity of infection (MOI), HepG2 cells were infected with AdCYP2C9 at MOI 0, 2.5, 5, 10, or 20 for 2 days. Diclofenac 4′-hydroxylase activity and CYP2C9 protein level were measured (Fig. 1). The activity and CYP2C9 protein level were increased MOI dependently in AdCYP2C9-infected cells, whereas they were not detected in AdGFP-infected cells at MOI 20. The highest activity and protein level were observed in cells infected with AdCYP2C9 at MOI 20, but the cells were slightly damaged (data not shown). At MOI 10, diclofenac 4′-hydroxylase activity was 0.957 ± 0.070 nmol/min/mg protein, a value that was higher than those in human hepatocytes reported in other reports (Supplemental Table 1). With HepG2 cells infected with AdCYP2C9 at MOI 10 for 1, 2, 3, or 5 days, the highest activity was observed after a 2-day infection, although the protein levels appeared to be similar after 2- to 5-day infections (Fig. 1B). From these results, AdCYP2C9 infection to HepG2 cells was performed at MOI 10 for 2 days in the subsequent experiments.

Effect of SiNrf2 on Nrf2 Protein Expression in Adenovirus-Infected HepG2 Cells. Our recent study demonstrated that CYP3A4-induced cytotoxicities of several drugs such as acetaminophen and flutamide were sensitively detected by Nrf2 knockdown (H. Hosomi, T. Fukami, A Iwamura, M. Nakajima, and T. Yokoi, manuscript submitted for publication). This study also used HepG2 cells transfected with siNrf2. Nrf2 protein expression in HepG2 cells was efficiently decreased by transfection of siNrf2 (26.8 ± 1.1 and 27.1 ± 2.0%, respectively), and the effect of siNrf2 was not affected by CYP2C9 overexpression (Fig. 1C).

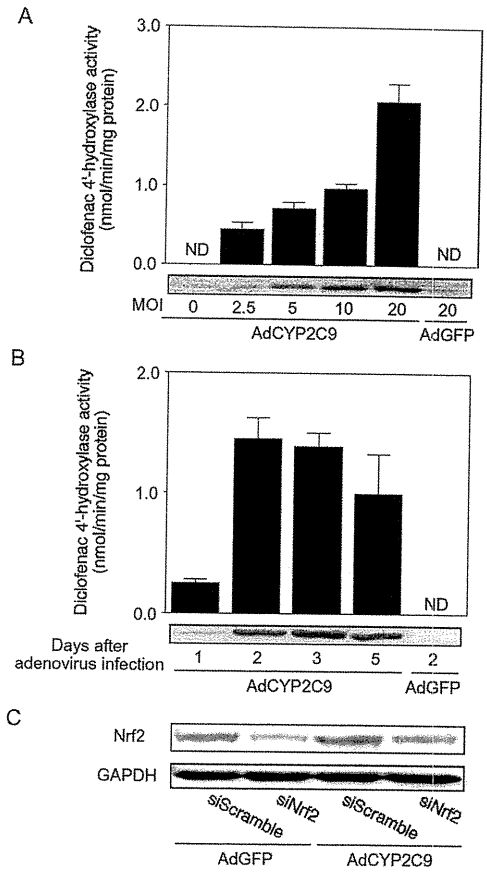

FIG. 1. MOI-dependent (A) and time-dependent (B) changes of diclofenac 4′-hydroxylase activity and CYP2C9 protein level in adenovirus (AdCYP2C9 or AdGFP)-infected HepG2 cells. HepG2 cells were infected with adenovirus for 2 days (A) or at MOI 10 (B). Diclofenac 4′-hydroxylase activity was measured as described under *Materials and Methods*. The CYP2C9 protein level was analyzed by immunoblotting using total cell homogenates from adenovirus-infected HepG2 cells, and the representative bands are demonstrated. Data are means ± S.D. (n = 3). C, Nrf2 protein level in HepG2 cells transfected with siScramble or siNrf2. HepG2 cells were infected with adenovirus (AdCYP2C9 or AdGFP) at MOI 10 for 2 days after a 24-h incubation with 10 nM siRNA. The relative band intensity of Nrf2 was normalized with the band intensity of GAPDH. Data are means ± S.D. (n = 3). **, $P < 0.01$ compared with AdGFP-infected groups transfected with siScramble. ND, not detected.

CYP2C9-Induced Cytotoxicity in HepG2 Cells Transfected with siNrf2. To investigate the CYP2C9-mediated metabolic activation of eight hepatotoxic drugs (benzbromarone, flutamide, fluvastatin, losartan, terbinafine, tienilic acid, valproic acid, and zolpidem), HepG2 cells infected with AdCYP2C9 at MOI 10 for 2 days were treated with drugs for 24 h. As a negative control, AdGFP was infected at MOI 10. To improve the sensitivity, HepG2 cells were transfected with siNrf2 24 h before adenovirus infection. Cytotoxicity was evaluated by WST-8 and ATP assays (Figs. 2 and 3). In the WST-8 assay, the viabilities of AdCYP2C9-infected cells were significantly decreased compared with those of AdGFP-infected cells by treatment with benzbromarone (10–40 μM), tienilic acid (100 and 200 μM), and losartan (25–100 μM) (Fig. 2). On the other hand, the viabilities of AdCYP2C9-infected cells were not different from those of AdGFP-infected cells by treatment with flutamide, fluvastatin, terbinafine, valproic acid, and zolpidem, except when treated with 100 μM fluvastatin. The ATP assay revealed a result similar to that of the WST-8 assay in that the viabilities of AdCYP2C9-infected cells were significantly decreased compared with those of AdGFP-infected cells by treatment with the benzbromarone (10–40 μM), tienilic acid

DMD DRUG METABOLISM AND DISPOSITION aspet

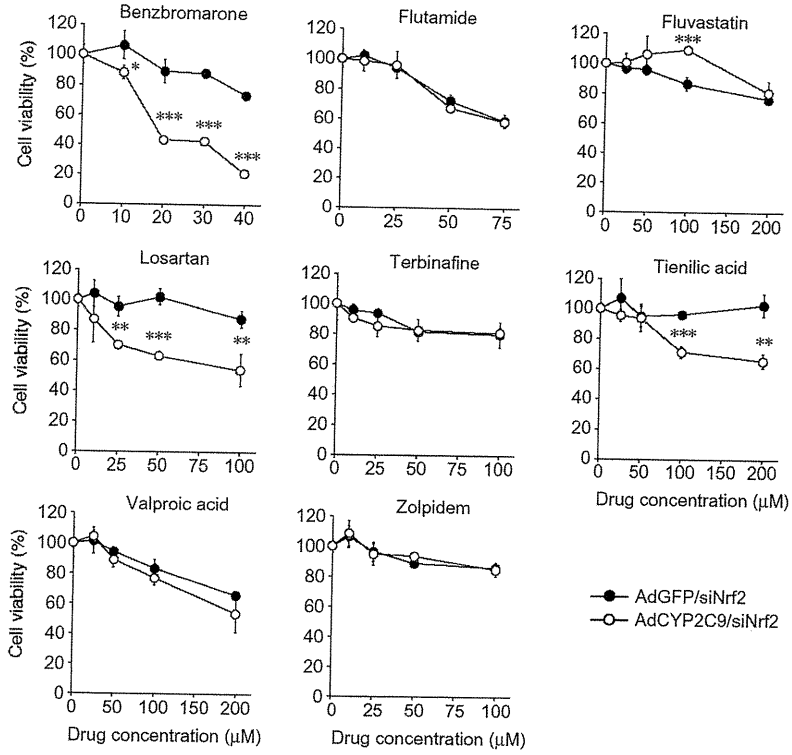

FIG. 2. CYP2C9-induced cytotoxicity in HepG2 cells transfected with siNrf2 (WST-8 assay). HepG2 cells were infected with adenovirus at MOI 10 for 2 days after a 24-h incubation with 10 nM siNrf2. Cell viability was measured by WST-8 assay after a 24-h treatment with the test drugs. Cell viability is expressed as a percentage of cells without drug treatment. Data are means ± S.D. ($n = 3$). *, $P < 0.05$; **, $P < 0.01$; ***, $P < 0.001$, compared with AdGFP-infected groups.

(50–200 μM), and losartan (10–100 μM) (Fig. 3). These results suggested that the benzbromarone-, tienilic acid-, and losartan-induced cytotoxicities are caused by the metabolic activation of CYP2C9.

CYP2C9-Induced Cytotoxicity in HepG2 Cells Transfected with siScramble. To investigate whether Nrf2-associated cytoprotective genes were involved in the benzbromarone-, tienilic acid-, and losartan-induced cytotoxicities mediated by CYP2C9, the cytotoxicity was evaluated with HepG2 cells transfected with siScramble instead of siNrf2 (Fig. 4). Terbinafine was used as a negative control. With the drugs except terbinafine, the viabilities of AdCYP2C9-infected cells were significantly decreased compared with those of AdGFP-

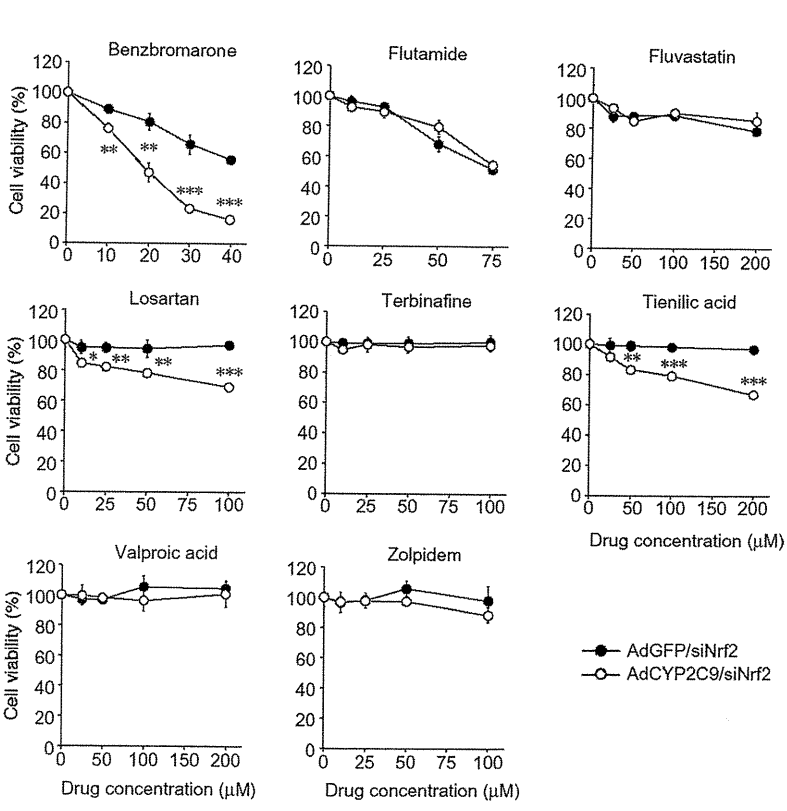

FIG. 3. CYP2C9-induced cytotoxicity in HepG2 cells transfected with siNrf2 (ATP assay). HepG2 cells were infected with adenovirus at MOI 10 for 2 days after a 24-h incubation with 10 nM siNrf2. Cell viability was measured by ATP assay after a 24-h treatment with the test drugs. Cell viability is expressed as a percentage of cells without drug treatment. Data are means ± S.D. ($n = 3$). *, $P < 0.05$; **, $P < 0.01$; ***, $P < 0.001$, compared with AdGFP-infected groups.

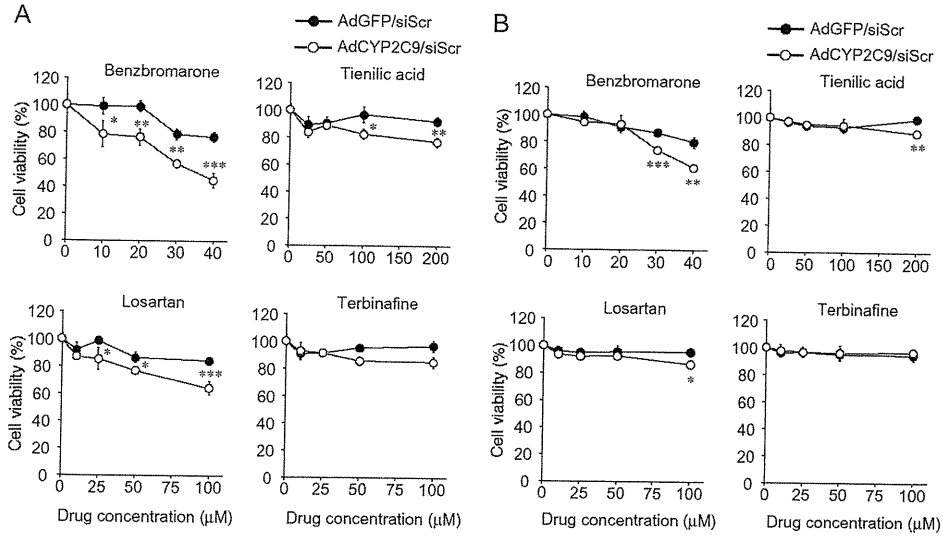

FIG. 4. CYP2C9-induced cytotoxicity in HepG2 cells transfected with siScramble. HepG2 cells were infected with adenovirus at MOI 10 for 2 days after a 24-h transfection with 10 nM siScramble. Cell viability was measured by the WST-8 assay (A) and the ATP assay (B) after a 24-h treatment with the test drugs. Cell viability is expressed as a percentage of cells without drug treatment. Data are means ± S.D. (n = 3). *, $P < 0.05$; **, $P < 0.01$; ***, $P < 0.001$, compared with AdGFP-infected groups.

infected cells, but the differences in the viabilities between AdGFP- and AdCYP2C9-infected cells transfected with siScramble were less than those of cells transfected with siNrf2.

Comparison of CYP2C9-Mediated Cytotoxicity between Losartan and Various Sartans. Because the cell-based assay system revealed that the losartan-induced cytotoxicity involved metabolic activation by CYP2C9, it was conceivable that other sartans with similar structures were also metabolically activated by CYP2C9. The viabilities of AdCYP2C9-infected cells were investigated by treatment with various sartans such as eprosartan, candesartan, irbesartan, olmesartan, telmisartan, and valsartan. However, no sartans other than losartan affected the cell viabilities (Fig. 5). Thus, among members of the sartan family, only losartan is associated with CYP2C9-mediated cytotoxicity.

Detection of Semicarbazide Adducts of Losartan. The semicarbazide adducts of losartan were investigated by the positive ion mode of LC-MS/MS. It was reported that CYP3A4 is involved in the metabolism of losartan (Stearns et al., 1995). However, no cytotoxicity of losartan was induced when the cells were infected with AdCYP3A4 constructed previously (Hosomi et al., 2010) instead of AdCYP2C9 (data not shown). Therefore, to detect adducts specifically generated by CYP2C9, losartan was incubated with CYP2C9 or CYP3A4 (negative control) Supersomes. As shown in Fig. 6, three semicarbazide adducts of losartan (S1, S2, and S3) were detected in the presence of CYP2C9 Supersomes by a precursor ion scan at m/z 494.2 ($[M + H]^+$). Because S3 was also detected when incubated with the CYP3A4 Supersomes, S3 was considered not to be involved in the CYP2C9-mediated cytotoxicity. Therefore, the subsequent study of S3 was not performed.

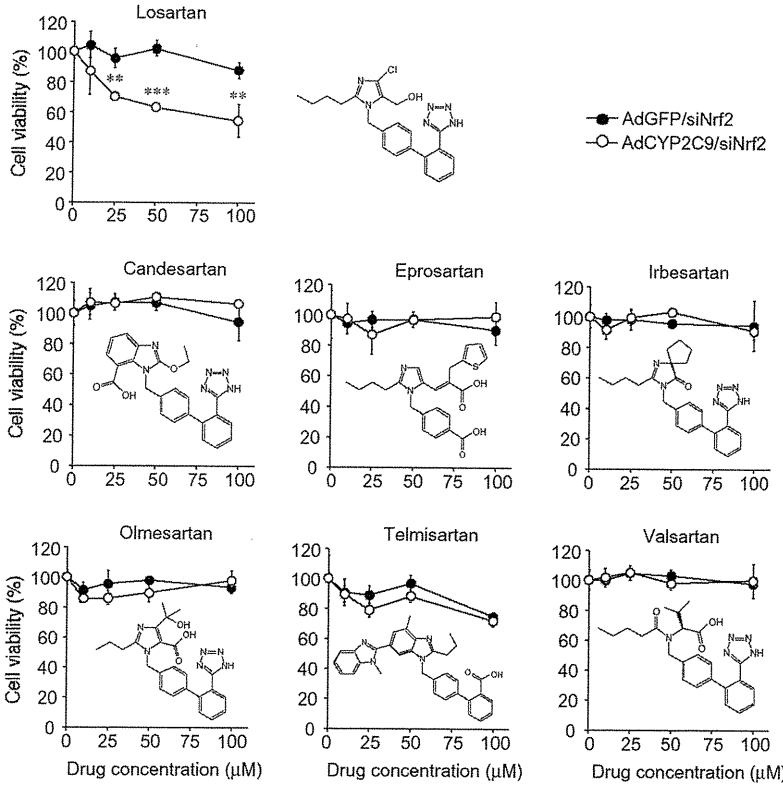

FIG. 5. Comparison of CYP2C9-mediated cytotoxicity between losartan and various sartans. HepG2 cells were infected with adenovirus at MOI 10 for 2 days after a 24-h transfection with 10 nM siNrf2. Cell viability was measured by the WST-8 assay after a 24-h treatment with the drugs. Cell viability is expressed as a percentage of cells without drug treatment. Data are means ± S.D. (n = 3). *, $P < 0.05$; **, $P < 0.01$, compared with AdGFP-infected groups.

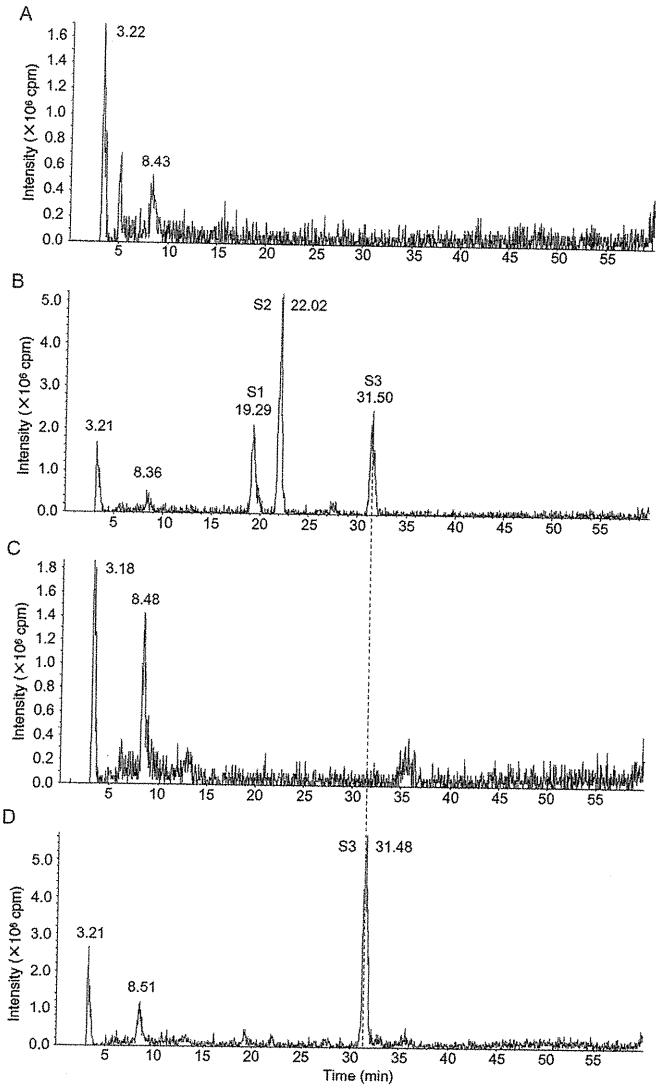

FIG. 6. Ion chromatograms from LC-MS/MS analysis of the semicarbazide adducts of losartan at *m/z* 494.2 ($[M + H]^+$). A, CYP2C9 Supersomes without semicarbazide. B, CYP2C9 Supersomes with semicarbazide. C, CYP3A4 Supersomes without semicarbazide. D, CYP3A4 Supersomes with semicarbazide. Incubation and LC-MS/MS conditions were as described under *Materials and Methods*.

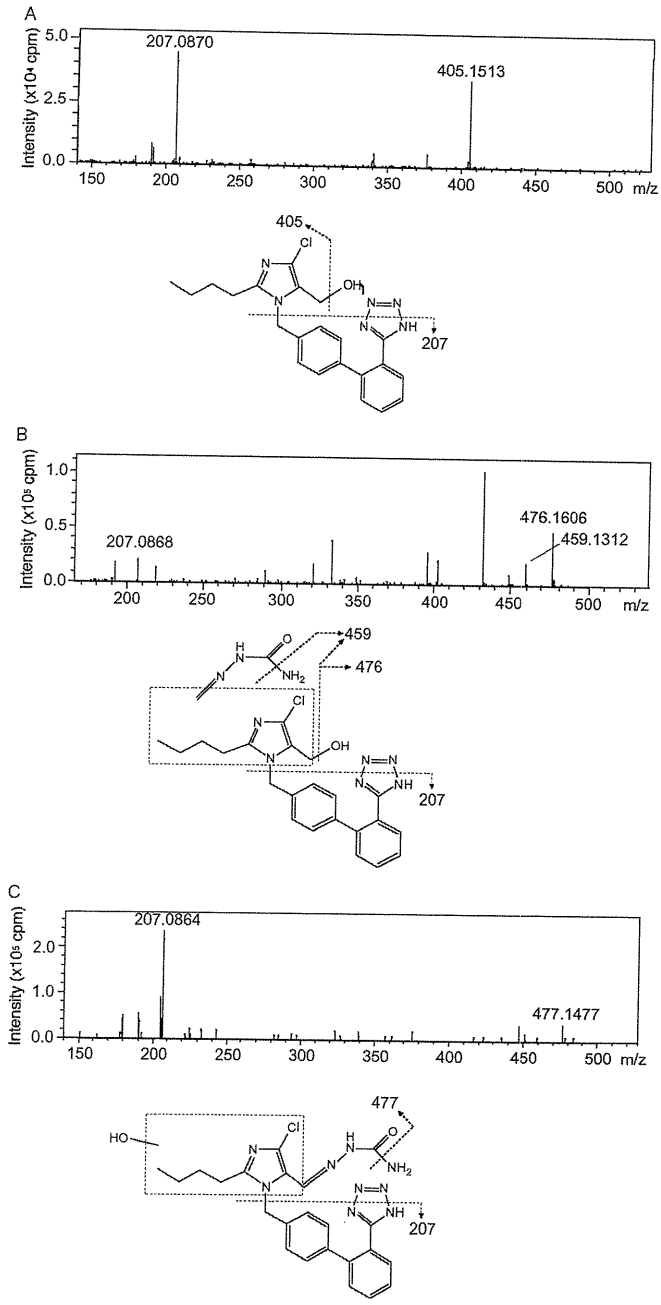

FIG. 7. Predicted structures of semicarbazide adducts of losartan and MS/MS spectra of the product ion obtained by collision-induced dissociation of (A) losartan at *m/z* 423.2 ($[M + H]^+$) and (B) S1 and (C) S2 at *m/z* 494.2 ($[M + H]^+$). The precursor ion at *m/z* 423.2 is semicarbazide adducts of losartan hydroxide. These spectra were scanned using LCMS-IT-TOF. Incubation and LCMS-IT-TOF conditions were as described under *Materials and Methods*.

Identification of Semicarbazide Adducts of Losartan. The structures of S1 and S2 were estimated by the positive ion mode of LCMS-IT-TOF (Fig. 7). The product ion mass spectrum of losartan exhibited a major fragment ion at *m/z* 405.1513 ($C_{22}H_{22}N_6Cl$) (Fig. 7A). The fragment ion at *m/z* 405.1513 was $[M + H - 18]^+$, indicating the losses of H_2O from alcohol group of losartan. The product ion mass spectrum of S1 exhibited two major fragment ions at *m/z* 476.1606 ($C_{23}H_{23}N_9OCl$) and *m/z* 459.1312 ($C_{23}H_2ON_8OCl$). The fragment ions at *m/z* 476.1606 and *m/z* 459.1312 were $[M + H - 18]^+$ and $[M + H - 35]^+$, indicating the losses of H_2O and NH_3 and H_2O, respectively. On the other hand, the product ion mass spectrum of S2 exhibited fragment ions at *m/z* 477.1477. The fragment ions at *m/z* 477.1477 were $[M + H - 17]^+$, indicating the loss of NH_3 from semicarbazide. Furthermore, the fragment ion at *m/z* 207.08 given from all three precursor ions indicated no conjugation with the biphenyl or tetrazole ring. The possible structures of S1 and S2 are shown in Fig. 7, B and C. *m/z* 207.08 indicated no conjugation with the biphenyl or tetrazole ring, and $[M + H - 18]^+$ indicated the losses of H_2O from alcohol group of losartan. Therefore, these two fragment ions detected in both losartan and S1 suggested that semicarbazide conjugates with another position, that is, somewhere in the imidazole ring or the adjacent butyl side chain. In contrast, $[M + H - 17]^+$ instead of $[M + H - 18]^+$ given from S2 suggested that a reactive metabolite conjugated with semicarbazide is a hydroxylated form of E3179, an aldehyde metabolite of losartan.

Discussion

In this study, we constructed an in vitro cell-based assay system to evaluate the hepatotoxicity mediated by CYP2C9 and performed a

cytotoxicity assay for drugs that have been known to cause hepatotoxicity. Benzbromarone and tienilic acid are converted to reactive metabolites by CYP2C9. In addition, six other hepatotoxic drugs, whose reactive metabolites generated by CYP2C9 have not been identified although CYP2C9 is involved in their metabolism, were evaluated by our cell-based assay system. According to O'Brien et al. (2006), the cytotoxicity assay was performed within the drug concentration of 30 times the maximal efficacious concentration or 100 μM. We found that the viabilities of AdCYP2C9-infected cells were significantly decreased compared with those of AdGFP-infected cells by treatments with benzbromarone, tienilic acid, and losartan, suggesting that the hepatotoxicity induced by these drugs involves metabolic activation by CYP2C9. Benzbromarone is metabolized via 6-hydroxybenzbromarone to the catechol by CYP2C9, followed by the oxidization of the catechol to a reactive *ortho*-quinone metabolite (McDonald and Rettie, 2007). Tienilic acid is metabolized via the sulfoxide to 5-hydroxytienilic acid by CYP2C9. This sulfoxide can form a covalent bond with CYP2C9 or other proteins. In rat, administration of tienilic acid in combination with the glutathione biosynthesis inhibitor, buthionine sulfoximine (BSO), induced a marked elevation of the serum alanine aminotransferase (ALT) level, but no increase in the serum ALT activity was observed in the presence of the P450 inhibitor, 1-aminobenzotoriazole (Nishiya et al., 2008). Thus, the mechanisms for the metabolic activation of these drugs have been well examined. However, to our knowledge, cell-based assays for assessment of the metabolic activations of these drugs have not been performed. The results obtained in our cell-based assay system were in agreement with several reports that CYP2C9 is involved in the metabolic activations of benzbromarone and tienilic acid. However, there have been no reports of the involvement of CYP2C9 in the cytotoxicity of losartan. It has been reported that losartan could form protein or glutathione adducts by incubation with human liver microsomes and/or human hepatocytes, suggesting the metabolic activation of losartan (Gan et al., 2009; Usui et al., 2009). The present study demonstrated for the first time that CYP2C9 was responsible for the metabolic activation of losartan. The concentrations at which the metabolic activation of losartan was observed were much higher than those in plasma in clinical practice. To predict the involvement of CYP2C9 in losartan-induced toxicity, the combination of our established cell-based assay with other studies is needed.

Sartans have generally been used as safe drugs in clinical practice, but there have been various reports of losartan-induced hepatotoxicity, which is categorized as hepatocellular injury (Tabak et al., 2002; Chang and Schiano, 2007). In some case reports, a rechallenge to losartan after ALT normalization caused hepatotoxicities again (Bosch, 1997; Tabak et al., 2002). However, the contribution of immunological factors to losartan-induced hepatotoxicity was unknown. Losartan is metabolized to the carboxylic acid metabolite E3174, which is pharmacologically more active than the parent compound, via the aldehyde metabolite E3179, which is an intermediate in the oxidation of losartan. These biotransformations are catalyzed by CYP2C9 and CYP3A4. In addition to this pathway, the monohydroxylation of the butyl side chain is also catalyzed by CYP2C9 (Stearns et al., 1995). The viability of HepG2 cells was not decreased by treatment of E3179 and E3174 (Supplemental Fig. 1), suggesting that they may not show cytotoxicity. In this study, two CYP2C9-specific semicarbazide adducts of losartan (S1 and S2) were detected (Figs. 6 and 7). From the fragment ions of S1 and S2, it was suggested that S2 was produced via E3179, but S1 was not (Fig. 8). The cytotoxicity of losartan induced by CYP2C9 was attenuated by the treatment with semicarbazide (Supplemental Fig. 2). Therefore, the possible reactive metabolites from S1 and S2 might be involved in the cytotoxicity. Furthermore, no significant decreases in cell viabilities were observed by treatment with various sartans (irbesartan, valsartan, candesartan, olmesartan, telmisartan, and eprosartan) other than losartan. Taken together, these results suggested that the side chains or a chloro group besides the imidazole ring that is unique to losartan is important for the losartan-induced cytotoxicity mediated by CYP2C9.

The CYP2C9-induced cytotoxicities of benzbromarone, tienilic acid, and losartan were enhanced by Nrf2 knockdown, suggesting that the genes regulated by Nrf2 are associated with detoxification of their cytotoxicities. In our recent study, CYP3A4-induced cytotoxicities of several drugs such as acetaminophen and flutamide were sensitively detected by Nrf2 knockdown (H. Hosomi, T. Fukami, A. Iwamura, M. Nakajima, and T. Yokoi, manuscript submitted for publication). In addition, it was demonstrated that *nrf2*(−/−) mice are more vulnerable to acetaminophen-induced liver injury, due in part to lower cellular thiol levels and decreased expression of detoxification enzymes (Enomoto et al., 2001). Thus, Nrf2 is considered to play a quite important role in the detoxification of hepatotoxic drugs. Among the genes regulated by Nrf2, there are various genes involved in glutathione synthesis, such as the glutamate cysteine ligase catalytic subunit, the glutamate cysteine ligase regulatory subunit, and glutathione synthetase (Copple et al., 2008). Glutathione is an important intracellular peptide that detoxifies reactive metabolites by conjugation (Lu, 1999). In fact, reactive *ortho*-quinone metabolites of benzbromarone generated by CYP2C9 can be trapped with glutathione (McDonald and Rettie, 2007). In addition, the presence of glutathione markedly decreased the level of covalent binding of tienilic acid to microsomal proteins (Bonierbale et al., 1999). From these backgrounds, we considered whether the cytotoxicity of losartan could be clearly observed in a cytotoxicity assay with HepG2 cells transfected with siRNA for γ-glutamylcysteine synthetase heavy chain or treated with BSO instead of being transfected with siNrf2. However, no significant decreases in cell viabilities were observed by either transfection of siRNA for γ-glutamylcysteine synthetase heavy chain or treatment with BSO (data not shown). These results suggested that glutathione conjugation was not required for the detoxification of losartan-induced cytotoxicity but that other detoxification enzymes regulated by Nrf2 would be involved. Therefore, semicarbazide was used as a trapping agent for the reactive metabolites of losartan in this study. Semicarbazide is a hard nucleophile, which will preferentially react with hard electrophiles, such as aldehydes (Chauret et al., 1995). Indeed, the cytotoxicity of losartan induced by CYP2C9 was attenuated by treatment with semicarbazide (Supplemental Fig. 2). Thus, it is conceivable that reactive metabolites trapped by semicarbazide are involved in the CYP2C9-induced cytotoxicity of losartan.

In the present study, CYP2C9-mediated metabolic activation was not observed with flutamide, fluvastatin, terbinafine, valproic acid, and zolpidem, which are suspected to be associated with hepatotoxicity (Karsenti et al., 1999; Thole et al., 2004; Chang and Schiano, 2007). Flutamide is hydrolyzed to 4-nitro-3-(trifluoromethyl)phenylamine (FLU-1), which is further metabolized to *N*-hydroxy FLU-1, which can cause hepatotoxicity in rat (Ohbuchi et al., 2009). The N-hydroxylation of FLU-1 is catalyzed by CYP2C9 as well as by CYP3A4 (Goda et al., 2006). In this study, flutamide-induced cytotoxicity could not be detected. One possibility is that the intracellular concentration of FLU-1 was low because of the low flutamide hydrolase activity in HepG2 cells, although it was not measured. Terbinafine is known to be metabolized by a wide range of P450 enzymes including CYP2C9, primarily through N-demethylation, deamination, and hydroxylation (Vickers et al., 1999). Among its metabolites, 7,7-dimethylhept-2-ene-4-ynal was considered to play a role in the pathogenesis of hepatotoxicity (Iverson and Uetrecht, 2001), but this

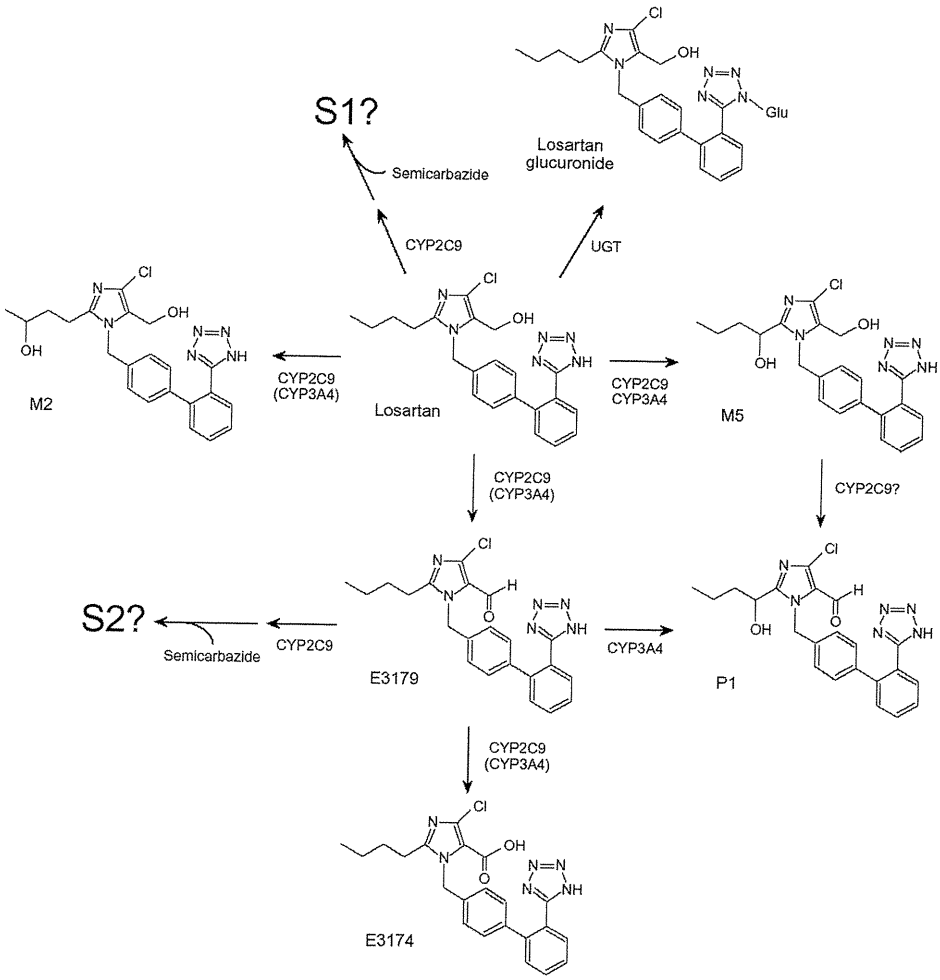

FIG. 8. Proposed metabolic pathways of losartan. UGT, UDP-glucuronosyltransferase.

metabolite is generated by CYP3A4, not by CYP2C9. That is why the cell viability was not affected by treatment with terbinafine in AdCYP2C9-infected cells. For the hepatotoxicity caused by valproic acid, the involvement of its reactive metabolites such as 4-ene-valproic acid and 2,4-diene-valproic acid was suggested (Baillie, 1988; Kassahun et al., 1991; Tang et al., 1995). CYP2C9 played a role in the formation of 4-ene-valproic acid (Sadeque et al., 1997), but no involvement of CYP2C9 in the cytotoxicity of valproic acid was observed in this study. It was reported that valproic acid produced a high level of covalent binding in rat liver after oral administration, although it did not bind to microsomal protein in vitro (Leone et al., 2007). Other factors as well as CYP2C9 might be responsible for the hepatotoxicity of valproic acid. The cytotoxicities of fluvastatin and zolpidem induced by CYP2C9 were not detected in the present study. Until now, the mechanisms of their cytotoxicities have been unknown. The present study suggested low involvement of CYP2C9 in their cytotoxicities, although it is responsible for the metabolism of these drugs (Fischer et al., 1999; Von Moltke et al., 1999).

In conclusion, we constructed a highly sensitive cell-based assay system to evaluate CYP2C9-mediated cytotoxicity and found for the first time that CYP2C9 is involved in the metabolic activation of losartan. This cell-based assay system would be useful in evaluating drug-induced cytotoxicity caused by human CYP2C9.

Acknowledgments

We thank Toru Usui and Dr. Takanori Hashizume (Pharmacokinetics Research Laboratories, Dainippon Sumitomo Pharma Co., Ltd., Osaka, Japan) for technical assistance with LC-MS/MS and LCMS-IT-TOF analyses and Brent Bell for reviewing the manuscript.

Authorship Contributions

Participated in research design: Iwamura, Fukami, Nakajima, and Yokoi.
Conducted experiments: Iwamura and Hosomi.
Contributed new reagents or analytic tools: Iwamura and Hosomi.
Performed data analysis: Iwamura and Fukami.
Wrote or contributed to the writing of the manuscript: Iwamura, Fukami, and Yokoi.

References

Baillie TA (1988) Metabolic activation of valproic acid and drug-mediated hepatotoxicity. Role of the terminal olefin, 2-*n*-propyl-4-pentenoic acid. *Chem Res Toxicol* **1**:195–199.
Bonierbale E, Valadon P, Pons C, Desfosses B, Dansette PM, and Mansuy D (1999) Opposite behaviors of reactive metabolites of tienilic acid and its isomer toward liver proteins: use of specific anti-tienilic acid-protein adduct antibodies and the possible relationship with different hepatotoxic effects of the two compounds. *Chem Res Toxicol* **12**:286–296.
Bosch X (1997) Losartan-induced hepatotoxicity. *JAMA* **278**:1572.
Chang CY and Schiano TD (2007) Review article: drug hepatotoxicity. *Aliment Pharmacol Ther* **25**:1135–1151.
Chauret N, Nicoll-Griffith D, Friesen R, Li C, Trimble L, Dubé D, Fortin R, Girard Y, and Yergey J (1995) Microsomal metabolism of the 5-lipoxygenase inhibitors L-746,530 and L-739,010 to reactive intermediates that covalently bind to protein: the role of the 6,8-dioxabicyclo[3.2.1]octanyl moiety. *Drug Metab Dispos* **23**:1325–1334.
Copple IM, Goldring CE, Kitteringham NR, and Park BK (2008) The Nrf2-Keap1 defence pathway: role in protection against drug-induced toxicity. *Toxicology* **246**:24–33.
Edwards RJ, Adams DA, Watts PS, Davies DS, and Boobis AR (1998) Development of a comprehensive panel of antibodies against the major xenobiotic metabolising forms of cytochrome P450 in humans. *Biochem Pharmacol* **56**:377–387.
Enomoto A, Itoh K, Nagayoshi E, Haruta J, Kimura T, O'Connor T, Harada T, and Yamamoto M (2001) High sensitivity of Nrf2 knockout mice to acetaminophen hepatotoxicity associated with decreased expression of ARE-regulated drug metabolizing enzymes and antioxidant genes. *Toxicol Sci* **59**:169–177.

Fischer V, Johanson L, Heitz F, Tullman R, Graham E, Baldeck JP, and Robinson WT (1999) The 3-hydroxy-3-methylglutaryl coenzyme A reductase inhibitor fluvastatin: effect on human cytochrome P-450 and implications for metabolic drug interactions. *Drug Metab Dispos* **27:**410–416.

Gan J, Ruan Q, He B, Zhu M, Shyu WC, and Humphreys WG (2009) In vitro screening of 50 highly prescribed drugs for thiol adduct formation—comparison of potential for drug-induced toxicity and extent of adduct formation. *Chem Res Toxicol* **22:**690–698.

Goda R, Nagai D, Akiyama Y, Nishikawa K, Ikemoto I, Aizawa Y, Nagata K, and Yamazoe Y (2006) Detection of a new *N*-oxidized metabolite of flutamide, *N*-[4-nitro-3-(trifluoromethyl)-phenyl]hydroxylamine, in human liver microsomes and urine of prostate cancer patients. *Drug Metab Dispos* **34:**828–835.

Greer ML, Barber J, Eakins J, and Kenna JG (2010) Cell based approaches for evaluation of drug-induced liver injury. *Toxicology* **268:**125–131.

Guengerich FP (2008) Cytochrome P450 and chemical toxicology. *Chem Res Toxicol* **21:**70–83.

Hewitt NJ and Hewitt P (2004) Phase I and II enzyme characterization of two sources of HepG2 cell lines. *Xenobiotica* **34:**243–256.

Hosomi H, Akai S, Minami K, Yoshikawa Y, Fukami T, Nakajima M, and Yokoi T (2010) An in vitro drug-induced hepatotoxicity screening system using CYP3A4-expressing and γ-glutamylcysteine synthetase knockdown cells. *Toxicol In Vitro* **24:**1032–1038.

Iverson SL and Uetrecht JP (2001) Identification of a reactive metabolite of terbinafine: insights into terbinafine-induced hepatotoxicity. *Chem Res Toxicol* **14:**175–181.

Karsenti D, Blanc P, Bacq Y, and Metman EH (1999) Hepatotoxicity associated with zolpidem treatment. *BMJ* **318:**1179.

Kassahun K, Farrell K, and Abbott F (1991) Identification and characterization of the glutathione and *N*-acetylcysteine conjugates of (*E*)-2-propyl-2,4-pentadienoic acid, a toxic metabolite of valproic acid, in rats and humans. *Drug Metab Dispos* **19:**525–535.

Koenigs LL, Peter RM, Hunter AP, Haining RL, Rettie AE, Friedberg T, Pritchard MP, Shou M, Rushmore TH, and Trager WF (1999) Electrospray ionization mass spectrometric analysis of intact cytochrome P450: identification of tienilic acid adducts to P450 2C9. *Biochemistry* **38:**2312–2319.

Lee WM (2003) Drug-induced hepatotoxicity. *N Engl J Med* **349:**474–485.

Leone AM, Kao LM, McMillian MK, Nie AY, Parker JB, Kelley MF, Usuki E, Parkinson A, Lord PG, and Johnson MD (2007) Evaluation of felbamate and other antiepileptic drug toxicity potential based on hepatic protein covalent binding and gene expression. *Chem Res Toxicol* **20:**600–608.

Li AP (2002) A review of the common properties of drugs with idiosyncratic hepatotoxicity and the "multiple determinant hypothesis" for the manifestation of idiosyncratic drug toxicity. *Chem Biol Interact* **142:**7–23.

Lu SC (1999) Regulation of hepatic glutathione synthesis: current concepts and controversies. *FASEB J* **13:**1169–1183.

McDonald MG and Rettie AE (2007) Sequential metabolism and bioactivation of the hepatotoxin benzbromarone: formation of glutathione adducts from a catechol intermediate. *Chem Res Toxicol* **20:**1833–1842.

Mizuno K, Katoh M, Okumura H, Nakagawa N, Negishi T, Hashizume T, Nakajima M, and Yokoi T (2009) Metabolic activation of benzodiazepines by CYP3A4. *Drug Metab Dispos* **37:**345–351.

Nishiya T, Kato M, Suzuki T, Maru C, Kataoka H, Hattori C, Mori K, Jindo T, Tanaka Y, and Manabe S (2008) Involvement of cytochrome P450-mediated metabolism in tienilic acid hepatotoxicity in rats. *Toxicol Lett* **183:**81–89.

O'Brien PJ, Irwin W, Diaz D, Howard-Cofield E, Krejsa CM, Slaughter MR, Gao B, Kaludercic N, Angeline A, Bernardi P, et al. (2006) High concordance of drug-induced human hepatotoxicity with in vitro cytotoxicity measured in a novel cell-based model using high content screening. *Arch Toxicol* **80:**580–604.

Ohbuchi M, Miyata M, Nagai D, Shimada M, Yoshinari K, and Yamazoe Y (2009) Role of enzymatic *N*-hydroxylation and reduction in flutamide metabolite-induced liver toxicity. *Drug Metab Dispos* **37:**97–105.

Park BK, Kitteringham NR, Maggs JL, Pirmohamed M, and Williams DP (2005) The role of metabolic activation in drug-induced hepatotoxicity. *Annu Rev Pharmacol Toxicol* **45:**177–202.

Rodríguez-Antona C, Donato MT, Boobis A, Edwards RJ, Watts PS, Castell JV, and Gómez-Lechón MJ (2002) Cytochrome P450 expression in human hepatocytes and hepatoma cell lines: molecular mechanisms that determine lower expression in cultured cells. *Xenobiotica* **32:**505–520.

Sadeque AJ, Fisher MB, Korzekwa KR, Gonzalez FJ, and Rettie AE (1997) Human CYP2C9 and CYP2A6 mediate formation of the hepatotoxin 4-ene-valproic acid. *J Pharmacol Exp Ther* **283:**698–703.

Stearns RA, Chakravarty PK, Chen R, and Chiu SH (1995) Biotransformation of losartan to its active carboxylic acid metabolite in human liver microsomes. Role of cytochrome P4502C and 3A subfamily members. *Drug Metab Dispos* **23:**207–215.

Tabak F, Mert A, Ozaras R, Biyikli M, Ozturk R, Ozbay G, Senturk H, and Aktuglu Y (2002) Losartan-induced hepatic injury. *J Clin Gastroenterol* **34:**585–586.

Tang W, Borel AG, Fujimiya T, and Abbott FS (1995) Fluorinated analogues as mechanistic probes in valproic acid hepatotoxicity: hepatic microvesicular steatosis and glutathione status. *Chem Res Toxicol* **8:**671–682.

Thole Z, Manso G, Salgueiro E, Revuelta P, and Hidalgo A (2004) Hepatotoxicity induced by antiandrogens: a review of the literature. *Urol Int* **73:**289–295.

Usui T, Mise M, Hashizume T, Yabuki M, and Komuro S (2009) Evaluation of the potential for drug-induced liver injury based on in vitro covalent binding to human liver proteins. *Drug Metab Dispos* **37:**2383–2392.

Vickers AE, Sinclair JR, Zollinger M, Heitz F, Glänzel U, Johanson L, and Fischer V (1999) Multiple cytochrome P-450s involved in the metabolism of terbinafine suggest a limited potential for drug-drug interactions. *Drug Metab Dispos* **27:**1029–1038.

Vignati L, Turlizzi E, Monaci S, Grossi P, Kanter R, and Monshouwer M (2005) An in vitro approach to detect metabolite toxicity due to CYP3A4-dependent bioactivation of xenobiotics. *Toxicology* **216:**154–167.

Von Moltke LL, Greenblatt DJ, Granda BW, Duan SX, Grassi JM, Venkatakrishnan K, Harmatz JS, and Shader RI (1999) Zolpidem metabolism *in vitro*: responsible cytochromes, chemical inhibitors, and *in vivo* correlations. *Br J Clin Pharmacol* **48:**89–97.

Yoshikawa Y, Hosomi H, Fukami T, Nakajima M, and Yokoi T (2009) Establishment of knockdown of superoxide dismutase 2 and expression of CYP3A4 cell system to evaluate drug-induced cytotoxicity. *Toxicol In Vitro* **23:**1179–1187.

Address correspondence to: Dr. Tsuyoshi Yokoi, Drug Metabolism and Toxicology, Faculty of Pharmaceutical Sciences, Kanazawa University, Kakuma-machi, Kanazawa 920-1192, Japan. E-mail: tyokoi@kenroku.kanazawa-u.ac.jp

Toxicology Letters 204 (2011) 17–24

Contents lists available at ScienceDirect

Toxicology Letters

journal homepage: www.elsevier.com/locate/toxlet

Estradiol and progesterone modulate halothane-induced liver injury in mice

Yasuyuki Toyoda[a], Taishi Miyashita[a], Shinya Endo[a], Koichi Tsuneyama[b], Tatsuki Fukami[a], Miki Nakajima[a], Tsuyoshi Yokoi[a,*]

[a] Drug Metabolism and Toxicology, Faculty of Pharmaceutical Sciences, Kanazawa University, Kakuma-machi, Kanazawa 920-1192, Japan
[b] Department of Diagnostic Pathology, Graduate School of Medicine and Pharmaceutical Science for Research, University of Toyama, Sugitani 930-0194, Toyama, Japan

ARTICLE INFO

Article history:
Received 27 January 2011
Received in revised form 29 March 2011
Accepted 30 March 2011
Available online 8 April 2011

Keywords:
Drug-induced liver injury
Halothane
Estradiol
Progesterone

ABSTRACT

Drug-induced liver injury (DILI) is one of the major problems in drug development and clinical drug therapy. In general, it is believed that women exhibit worse outcomes from DILI than men. It is known that halothane (HAL), an inhaled anesthetic, rarely induces severe liver injury. The risk factors for severe HAL-induced liver injury (HILI) are female sex, genetics and adult age. To investigate the underlying mechanism by which women are more susceptible to HILI, we focused on two major female sex hormones, estradiol (E2) and progesterone (Prog). In this study, we first found that pretreatment of mice with E2 attenuated HILI, whereas pretreatment with Prog exacerbated HILI. E2 and Prog had no effects on the degree of metabolic activation, the ratio of GSH/GSSG or oxidative stress in the liver. We observed higher numbers of neutrophils infiltrated into the liver and increased hepatic mRNA levels of proinflammatory cytokines, tumor necrosis factor (TNF) α, interleukin (IL)-1β and IL-6 and chemokines, CXCL1 and CXCL2 by pretreatment with Prog, whereas E2 pretreatment resulted in the opposite effects. These results suggest that E2 and Prog play a critical role in HILI via immune-related responses and female sex hormone balance might represent a risk factor for HILI.

1. Introduction

The occurrence of drug-induced liver injury (DILI) can be a major problem in all phases of clinical drug development. In most cases, the mechanisms of hepatotoxicity are unknown, but it is likely to arise from complex interactions among drugs, genetic, age, gender, disease and environmental factors (Chalasani and Björnsson, 2010; Li, 2002). In general, women are more susceptible to DILI than men. Seventy-eight percent of DILI cases occur in women, and a significantly greater number of women show hepatocellular DILI than men (Ostapowicz et al., 2002; De Valle et al., 2006; Björnsson and Olsson, 2005). In contrast, some reports described that there was no significant gender difference in the incident rates of DILI (Lucena et al., 2009; Andrade et al., 2005). However, it was also reported that patients with severe DILI who underwent liver transplantation in the US were more frequently women (76%) and that nearly 90% of patients with fluminant liver injury from DILI were women. Thus, women appear to be at greater risk of developing severe DILI (Lucena et al., 2009; Andrade et al., 2005; Russo et al., 2004), but it is not clear why women exhibit the worst outcomes in DILI.

Women elicit more vigorous cellular and humoral immune reactions, and suffer in greater numbers from autoimmune disease than men (Ansar et al., 1985; Ostensen, 1999). There is also evidence that the immune system is regulated by the circulating levels of sex steroid hormones, estradiol (E2), progesterone (Prog), and testosterone (Grossman, 1985). It was also reported that E2 inhibits proinflammatory cytokine production by murine peritoneal macrophages and mononuclear cells in vitro, whereas Prog may counteract this effect of E2 (Huang et al., 2008; Yuan et al., 2008). However, there has been little information concerning the involvement of female sex hormones in DILI.

Halothane (HAL) is an inhaled anesthetic that causes asymptomatic increases of plasma transaminases in approximately 20% of patients and severe liver injury in a small percentage of patients (Ray and Drummond, 1991). Risk factors for severe halothane-induced liver injury (HILI) are female sex, adult age, genetics, and multiple halothane exposures (Inman and Mushin, 1974; Cousins et al., 1989). HAL is metabolized to trifluoroacetyl (TFA)-chloride by cytochrome P450 (CYP) 2E1 and covalent binding to proteins and lipids. It has been suggested that TFA-adduct or halothane-modified macromolecules may be an initiating event for an immune response (Bourdi et al., 2001; Njoku et al., 1997; Gut et al., 1993). Recent studies indicate the mechanism of HILI involves immune responses such as neutrophils, IL-17 and natural killer cells (You et al., 2006; Kobayashi et al., 2009; Cheng et al., 2010).

Recently, a new mouse model of HILI was established and gender differences in the degree of HILI were suggested (You et al.,

* Corresponding author. Tel.: +81 76 234 4407; fax: +81 76 234 4407.
E-mail address: tyokoi@kenroku.kanazawa-u.ac.jp (T. Yokoi).

0378-4274/$ – see front matter © 2011 Elsevier Ireland Ltd. All rights reserved.
doi:10.1016/j.toxlet.2011.03.031